Physics – Uspekhi **39** (12) 1243 – 1272 (1996)

REVIEWS OF TOPICAL PROBLEMS PACS number: 02.70.Lq

Monte Carlo method in nonlinear statistical optics

V P Kandidov

Contents

Abstract. The state of the art of the Monte Carlo studies on randomly modulated optical waves in regular and randomly inhomogeneous nonlinear media is reviewed. A wide range of phenomena dealt with in nonlinear statistical optics are discussed, including self-phase noise pulse modulation, the self-action of partially coherent beams, the formation and instability of solitons, stimulated Raman scattering, intensive light beams in a turbulent atmosphere, and adaptive radiation focusing. Special attention is given to the justification of the phase screen model for a randomly inhomogeneous nonlinear continuum, and the numerical simulation of random light fields is discussed in detail.

1. Introduction

Nonlinear statistical optics encompasses a wide range of phenomena related to the nonlinear conversion, propagation, and generation of light waves. Among its problems are analysis of the effect of radiation fluctuations and irregularity of a medium on the efficiency of nonlinear processes and a study of the statistics of the light field in the case of nonlinear interaction with a medium. Partial coherence of the pump wave confines the efficiency of processes of harmonic generation, parametric frequency conversion of light, and stimulated Raman scattering [1]. Nonlinear effects in solid-state lasers result in the formation of ultrashort light pulses [2] and splitting of the light beam into filaments because of the small-scale self-focusing [3]. The simultaneous manifestation of nonlinearity and inhomogeneity of the active medium in flowing gas CO_2 lasers causes an increase in the divergence of radiation and pulsations of the output power [4]. As the laser beam propagates through a medium, fluctuations of the optical parameters of the medium result in perturbations of the light field whose development is governed by nonlinear effects. In the atmosphere, these are the effects of thermal self-action, breakdown, and nonlinear absorption in aerosols, which severely restrict the ultimate parameters of devices for laser probing and location [5].

Analysis of the nonlinear interaction between random waves is of interest both for modern optics and acoustics, radiophysics, and plasma theory. Stochastic wave processes in nonlinear media reflect the general regularities of transformation of spatial, temporal, and spectral parameters of the dynamic fields. These processes include, for example, the appearance of the turbulence in a plasma [6] and in shock sound waves [7 – 9] as well as the development of fluctuations in the intense light field in the atmosphere [10].

1.1 'Radiation – medium' system

In the case of stochastic nonlinear waves, it is important that their fluctuations and fluctuations of the parameters of a medium affect each other. In other words, the radiation field and the medium form a nonlinear distributed system with a closed feedback loop. When incoherent waves hit the regular medium, the nonlinear system is excited by fluctuations of the radiation. These fluctuations induce in the nonlinear medium the random field of perturbations, from which both the regular and fluctuative components of the waves are scattered. When the coherent wave is incident on the random (randomly inhomogeneous) medium, the parametric excitation of the 'radiation – medium' system takes place. In this case, scattering of the wave by inhomogeneities of the medium gives rise to its fluctuations, which in turn induce random perturbations in the medium.

Parametric scattering of the regular component of the wave by random perturbations induced in the medium results in energy transfer from this component to the fluctuation component. For this reason, fluctuations of the field and

V P Kandidov Physics Department, M V Lomonosov Moscow State University, Vorob'evy gory, 119899 Moscow, Russia
Tel. (7-095) 939-30-91
E-mail: kandidov@fort.phys.msu.su

Received 10 October 1996
Uspekhi Fizicheskikh Nauk **166** (12) 1309 – 1338 (1996)
Translated by M N Sapozhnikov, edited by A Radzig

medium can increase with time and space upon propagation of the wave in a nonlinear medium, i.e. the 'radiation – medium' system becomes unstable. Scattering of the fluctuation component of the wave by perturbations of the medium induced by this wave is equivalent to the closure of the feedback loop applied to fluctuations in the 'radiation – medium' system. This results in the transformation of the space – time statistics of radiation fluctuations in the nonlinear medium.

The study on statistics of the randomly modulated optical radiation in nonlinear media is one of the most complex problems of modern optics and laser physics. Theoretical treatment of statistical problems of nonlinear optics is performed by means of various analytic methods [1, 5, 11, 12]. However, the potentialities of analytic methods for studying the problems of nonlinear statistical optics are not great. This is explained by the fact that mean parameters of a random light field, i.e. the field moments, in the nonlinear medium are connected by an infinite chain of the differential equations, which can be completed only in the case of rather strong restrictions imposed on the field statistics, the level of field fluctuations, and the mutual correlation between perturbations in a radiation field and medium. Such assumptions correspond in fact to the breaking of feedback between fluctuations of the light field and medium in the nonlinear 'radiation – medium' system. Thus, in the perturbation methods the linearization is used which assumes that the fluctuation component ξE_0 of the field is small as compared to the regular component E_0 ($\xi \ll 1$) [11 – 14]. For this reason, first, the contribution of the fluctuation intensity $|\xi E_0|^2$ to the formation of medium random perturbations $\varepsilon_{\rm nl}$ is not taken into account and, second, scattering of field fluctuations ξE_0 by induced perturbations $\varepsilon_{\rm nl}$ is also neglected.

In studies based on the equations for the field moments, the assumption is used either that the normal distribution of fluctuations of the light wave is retained [1, 15, 16] or that fluctuations of the radiation and medium are statistically independent [11]. These assumptions allow one to uncouple joint moments for fluctuations of the field and medium and thus to obtain a closed system of equations for the moments of a light field. This system is commonly solved by using the nonaberrational approximation, which assumes that the field under study is statistically stationary, homogeneous, and isotropic. The assumption about conservation of the initial statistics of the light field is physically acceptable in the case of a weak nonlinearity. In this event, linear wave processes of diffraction and dispersion dominate over the nonlinear conversion of the wave. The assumption about statistical independence of the field fluctuations from those of the medium is valid under the conditions when inertial and nonlocal properties of a nonlinear medium response are manifested. Thus, upon thermal self-action of the light beam whose radius is much greater than the scale of random inhomogeneities of the field and medium, the fluctuations induced in the medium are rapidly smoothed because of the thermal conductivity, and the nonlinear refraction is mainly determined by an average temperature field [11, 17].

The initial statistical problem in the method of path integration is reduced to the continual integral equation, which can be solved by using the iteration procedure [18, 19]. In practice, only zero iteration can be performed, which corresponds to the approximation of the specified channel or specified intensity. The specified channel approximation, as the assumption of the statistical independence pertaining to fluctuations of the light field and medium, breaks virtually the feedback in fluctuations in the closed nonlinear 'radiation – medium' system.

Analysis of the averaged parameters of radiation based on the equations for the intensity moments is quite efficient [20, 21]. This approach, which is commonly referred to as the method of moments, provides the adequate accuracy if the light field is close to the statistically stationary and homogeneous field, which is valid in the case of a weak nonlinearity.

1.2 Numerical experiment in nonlinear statistical optics

With the advance of computing methods in studies on the interaction of coherent waves [22 – 24] it became possible to apply these methods to statistical problems of nonlinear optics. The performance of statistical testing with random light fields in nonlinear media with regular and randomly inhomogeneous parameters opens up fundamentally new opportunities in nonlinear statistical optics.

The method of statistical tests, which is also called the Monte Carlo method (MCM), is commonly defined as the procedure of constructing a random variable whose mathematical expectation is sought for [25]. The MCM in nonlinear statistical optics consists in the numerical computer simulation of stochastic light fields whose moments and distribution functions are the required statistical parameters of radiation in a nonlinear medium. The statistical analysis of an ensemble of random light fields allows one to perform, based on a unified approach, the combined study of radiation parameters in a nonlinear medium [10, 26, 27]. Numerical computer experiments with random light fields permit one to study the mechanism of the development of their instability, to investigate statistical and integrated parameters of radiation, to find the laws that govern the fluctuation distribution, to obtain critical values of the propagation parameters, and, finally, to determine the domain of applicability of various assumptions that are used in analytic estimates. The MCM also permits the calculation of the optimum parameters of particular lasers operating under actual experimental conditions.

2. Monte Carlo method in nonlinear optics of random media

2.1 Monte Carlo procedure

2.1.1 Corpuscular approach. In nonlinear optics, the MCM has been apparently first applied to studies on generation of the ultrashort light pulses. The analysis was based on the fluctuation model proposed in Refs [28, 29] and developed in Ref. [30]. This model considers the evolution of statistically independent fluctuations of the spontaneous emission from a laser under the conditions of their amplification by an active medium and selection by a nonlinear absorber. 'Computer oscillograms' of the laser burst were used for studying the dynamics of formation of the ultrashort pulses in a solid-state laser with a bleaching filter and also in a Raman fiber laser [31, 32].

The algorithms of MCM have been best developed in neutron physics. The direct application of these algorithms to the optical problems results in the corpuscular model, in which the propagation of light is treated as the Markov chain of random collisions of photons with molecules of a substance (Fig. 1a) [33]. The angular distribution and polarization of the scattered radiation [34], random broadening and walk of the

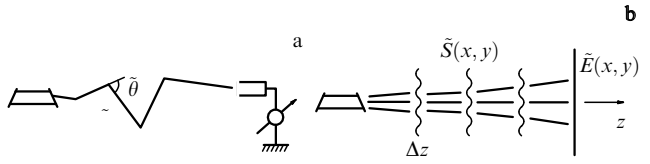

Figure 1. Models of radiation propagation in a random medium: (a) corpuscular model, (b) phase screen model.

light beams [35], the visibility of a scattering object [36], and the nonspherical aerosol modulation transfer functions [37] are investigated over an ensemble consisting of several thousands of random trajectories of a photon.

Close to the corpuscular model is the approach based on geometrical optics. The latter has been used for calculating the random propagation of light beams in the atmosphere represented by randomly located spherical vortices of various scales with different profiles of the refractive index [38], and also the propagation of the sound waves in a submarine acoustic channel with a random field of internal waves [39].

2.1.2 Phase screen model. In nonlinear optics, the MCM started from the wave concept is more promising. In this method, in contrast to simulation of elementary events of the light interaction with the matter, the wave process of the stochastic radiation propagation through a random nonlinear medium is considered. The wave model is based on the parabolic theory of diffraction and dispersion, and represents the generalization of the Markov approximation in the optics of random media to the nonlinear case. Such an approach is acceptable for stochastic radiation, provided the scales of the field and medium inhomogeneities greatly exceed the wavelength λ. The radiation possesses a narrow spatial spectrum, the directivity diagram of light scattered by inhomogeneities of the medium being strongly extended along the propagation direction. This allows one to neglect the backscattering, which corresponds to the description of the radiation propagation in a random medium by the Markov process. In the Markov approximation, the light wave passes successively through the layers of a random medium [40].

The phase screen model (PSM) represents the development of these concepts. In this model, a random continuum is replaced by a chain of scattering screens (Fig. 1b). In the case of a nonlinear random medium, the PSM comprises a chain of alternating screens, some of which simulate 'intrinsic' inhomogeneities of the medium and the others simulate inhomogeneities induced by a random light field. Between the screens, diffraction and dispersion of the radiation scattered forward takes place.

The PSM refers to a quite general approach to the study of the waves in random media. The description of a continuum with large-scale inhomogeneities by means of the sequence of layers has been used in the local method of small perturbations [41, 42]. The PSM is widely applied for studying fluctuations of the acoustic signal in the sound ocean channel, seismic waves in the Earth's crust, electromagnetic waves in an ionospheric and cosmic plasma, and light waves in the turbulent atmosphere [43].

The simplest model containing a single phase screen reflects the main properties of the wave field in a random continuum and allows one to perform analytic calculations of many statistical parameters of this field. The possibility of analysis of the wave diffraction in a thick slab of a random medium by means of the single-phase screen model has been apparently first considered in [44]. The theory of the wave diffraction behind a thin screen with a random phase and the amplitude modulation was presented at length within the spectral representation in a fundamental review article [45].

A single phase screen describes most adequately the scattering of waves in a thin layer of a medium when fluctuations of the light field develop behind the layer. This situation corresponds to the propagation of electromagnetic waves through the ionosphere [45]. The conditions of applicability of the thin phase screen model to ionospheric problems were considered in [46]. Later, it was shown [47] that this model when applied to the ionosphere shows a good fit to calculated results obtained by the method of smooth perturbations. The one-dimensional phase screen was used for studying the spectrum of the intensity distribution density under conditions of large fluctuations of the radio waves scattered in the ionosphere and for interpreting the flicker effect observed for broadband signals from satellites [48].

The simple single-phase screen model is used for theoretical analysis of various statistical problems in the wave theory. In [49, 50], strong fluctuations of the intensity of the plane wave scattered by a single-scale screen were considered, and in [51], those scattered by a screen with a broad spectrum of spatial phase fluctuations. The approximation of nonlinear geometrical acoustics was employed in analytic studies of the mean values and distributions functions and probabilities of fluctuations of the amplitude of shock fronts for the wave of an arbitrary profile scattered by a one-dimensional phase screen [52]. In [53], the estimate was made of the time of pulse propagation from a radiator to a receiver, with a phase screen located between them. It was found that the intensity-weighted mean time of the signal arrival to the receiver turned out to be longer than the mean time calculated without taking into account the intensity weight.

An error in the representation of a continuous layer of the inhomogeneous medium by a single phase screen was analyzed in [54] started from the numerical solution to the equation for the fourth moment of a signal. It was found that for a layer whose thickness is smaller than the external scale L_0 of the inhomogeneity, the variances of intensity fluctuations are the same for a continuum and an infinitely thin screen. For the layer thickness exceeding L_0, the phase screen substantially increases the intensity fluctuations in the absence of saturation. The error in the model considerably decreases when the screen is located in the middle of the route.

The chain PSM reproduces the properties of a random continuum much more accurately. The problem of the adequacy of PSM to a continuum is of fundamental importance [43]. In [55], it was shown in particular that the variance of the field phase in the case of weak fluctuations tends to the analytic estimate within the approximation of the method of smooth perturbations. The identity of the expressions for the fourth field moment represented by the convolution for a continuum and that obtained for a chain of phase screens has been demonstrated in [56].

The PSM for a nonlinear random medium is based on the following assumptions:

(1) Perturbations of optical properties of a medium caused by its irregularity and nonlinearity, are additive. This means that the dielectric constant $\bar{\varepsilon}_\Sigma$ of the medium, which is generally complex, can be represented in the form

$$\bar{\varepsilon}_\Sigma = \bar{\varepsilon} + \bar{\varepsilon}_{\mathrm{nl}} + \bar{\tilde{\varepsilon}}\,, \tag{2.1}$$

where $\bar{\varepsilon}$ is the unperturbed dielectric constant, $\bar{\varepsilon}_{\rm nl}$ and $\tilde{\bar{\varepsilon}}$ are the contributions to the dielectric constant resulted from nonlinearity and irregularity of the medium, respectively. This assumption is acceptable for dielectrics, optical fibres, atmospheric and oceanic optics.

(2) The medium is weakly nonlinear and weakly inhomogeneous:

$$\bar{\varepsilon}_{\rm nl}, \quad \tilde{\bar{\varepsilon}} \ll \bar{\varepsilon}\,. \tag{2.2}$$

(3) The spatial and time spectra of the radiation are narrow:

$$\frac{k_\perp}{k_z}\,, \quad \frac{\Delta\omega}{\omega_0} \ll 1\,, \tag{2.3}$$

where $k_\perp$ is the projection of the wave vector in the plane perpendicular to the direction of propagation along the Oz-axis, $\Delta\omega$ is the width of the frequency spectrum. Inequalities (2.3) mean that scales of the spatial ($r_{\rm c}$) and time coherence $\tau_{\rm c}$ of the field considerably exceed the wavelength λ and period T of the wave:

$$\frac{r_{\rm c}}{\lambda}\,, \quad \frac{\tau_{\rm c}}{T} \gg 1\,. \tag{2.4}$$

(4) Perturbations of the random medium are large-scale in the space and are slowly varying in time:

$$\frac{l_{\tilde{\varepsilon}}}{\lambda}\,, \quad \frac{\tau_{\tilde{\varepsilon}}}{T} \gg 1\,, \tag{2.5}$$

where $l_{\tilde{\varepsilon}}$ and $\tau_{\tilde{\varepsilon}}$ are the spatial and time scales of 'intrinsic' inhomogeneities of the medium.

In a weakly nonlinear medium whose perturbations meet conditions (2.5), the space–time spectrum of the light field $E(\mathbf{r}, z, t)$ is slowly enriched, the wave remains to be weakly divergent and quasi-monochromatic and satisfies inequalities (2.4). As a result, inhomogeneities induced by the field in the medium can be considered as large-scale and slowly varying:

$$\frac{l_{\rm nl}}{\lambda}\,, \quad \frac{\tau_{\rm nl}}{T} \gg 1\,. \tag{2.6}$$

This allows one to use the parabolic approximation of the theory of diffraction and dispersion for a stochastic light field in a nonlinear random medium [40, 57]. The complex amplitude $\widetilde{E}(\mathbf{r}, z, t)$ of the field obeys the equation

$$2{\rm i}k_0\,\frac{\partial\widetilde{E}}{\partial z} = \Delta_\perp\widetilde{E} - k_0\,\frac{\partial^2 k}{\partial\omega^2}\,\frac{\partial^2\widetilde{E}}{\partial\eta^2} + k_0^2\,\frac{\varepsilon_{\rm nl}+\tilde{\varepsilon}}{\varepsilon}\,\widetilde{E} - {\rm i}k_0\alpha_\Sigma\widetilde{E}\,, \tag{2.7}$$

where $\eta = t - z/u_{\rm gr}$ is the time in the accompanying coordinate system, $k_0 = \omega\sqrt{\varepsilon\varepsilon_0\mu_0}$ is the wave number for the unperturbed medium, and ε_0 and μ_0 are the dielectric constant and magnetic permeability, respectively, $\varepsilon = {\rm Re}\,\bar{\varepsilon}$, $\varepsilon_{\rm nl} = {\rm Re}\,\bar{\varepsilon}_{\rm nl}$, and $\tilde{\varepsilon} = {\rm Re}\,\tilde{\bar{\varepsilon}}$.

The attenuation coefficient α_Σ is described by the expressions

$$\alpha_\Sigma = \alpha + \alpha_{\rm nl} + \tilde{\alpha}\,, \quad \alpha = -k_0\,{\rm Im}\,\bar{\varepsilon}\,,$$
$$\alpha_{\rm nl} = -k_0\,{\rm Im}\,\bar{\varepsilon}_{\rm nl}\,, \quad \tilde{\alpha} = -k_0\,{\rm Im}\,\tilde{\bar{\varepsilon}}\,. \tag{2.8}$$

The perturbations $\bar{\varepsilon}_{\rm nl}$ induced in the medium are determined from constitutive equations whose specific form can be obtained from analysis of the radiation interaction with the medium. Such an analysis has been performed for problems of nonlinear atmospheric optics in Ref. [58].

In the case of nonlinearity caused by the electronic polarizability, i.e. by the orientation Kerr effect, the constitutive equation for $\varepsilon_{\rm nl}$ takes the form [57, 59]

$$\tau_{\rm nl}\,\frac{\partial\varepsilon_{\rm nl}}{\partial t} + \varepsilon_{\rm nl} = \varepsilon_2 EE^*\,, \tag{2.9}$$

where ε_2 is the coefficient attached to the cubic term in the expansion of the nonlinear polarizability in the field, and $\tau_{\rm nl}$ is the time of establishment of the nonlinear response. In the case of the isobaric thermal self-action [5]:

$$\left[\rho C_p\left(\frac{\partial}{\partial t} + \mathbf{v}\boldsymbol{\nabla}\right) - \varkappa\Delta\right]\varepsilon_{\rm nl} = \frac{\partial\varepsilon}{\partial T}\,\alpha_{\rm abs} I\,, \tag{2.10}$$

where $\widetilde{I} = (cn_0\varepsilon\varepsilon_0/2)\widetilde{E}\widetilde{E}^*$ is the radiation intensity.

Under conditions of the nonlinear light absorption, the system of constitutive equations also describes a change in the coefficient $\alpha_{\rm nl}$. For example, upon bleaching of an aqueous aerosol, $\alpha_{\rm nl}$ is determined from a chain of kinetic equations for the moments of the size distribution function of particles [60].

Equation (2.7) is considered, simultaneously with constitutive equations, for a given field $\widetilde{E}(\mathbf{r}, 0, t)$ in the plane $z = 0$ of the transmission aperture:

$$\widetilde{E}(\mathbf{r}, 0, t) = \widetilde{E}_0(\mathbf{r}, t)\,. \tag{2.11}$$

The field $\widetilde{E}_0(\mathbf{r}, t)$ is a regular field for a coherent source and a stochastic field with the specified spectrum $\Phi_E(\vec{\varkappa}, \omega)$ for a partially coherent source. The random field $\tilde{\bar{\varepsilon}}(\mathbf{r}, z, t)$ of 'intrinsic' fluctuations of the dielectric constant of a medium is determined by its space–time spectrum $\Phi_\varepsilon(\vec{\varkappa}, \omega)$, which is assumed to be known.

According to [40], one can more strictly define the range of applicability of parabolic equation (2.7) for analysis of the self-action of stochastic light fields in the random nonlinear media. Along with inequalities (2.4)–(2.6) characterizing the large scale of inhomogeneities of the medium, the following conditions should be also satisfied:

$$l_{\tilde{\varepsilon}}^4, \quad l_{\rm nl}^4, \quad r_{\rm c}^4 \gg \lambda^3 z; \qquad \tau_\varepsilon^3, \quad \tau_{\rm nl}^3, \quad \tau_{\rm c}^3 \gg \frac{\partial^3 k}{\partial\omega^3}\,z\,, \tag{2.12}$$

which determine the validity of parabolic approximations in the diffraction and dispersion theories:

$$\alpha_\Sigma\lambda \ll 1, \quad \pi^2 k_0^2 z\int_{k\sqrt{2}}^{k}\Phi(\varkappa)\varkappa\,{\rm d}\varkappa \ll 1\,, \tag{2.13}$$

which corresponds, in turn, to a small absorbed and backscattered energy.

Conditions (2.5) and (2.6) allow one to extend the Markov approximation to the nonlinear case and to use the PSM for studying waves in random nonlinear media. The complex amplitude of an electric field in the observation plane is determined from a numerical experiment based on the PSM. This is equivalent to measurements of the amplitude and phase of the light field in a nonlinear medium with a known statistics of the incident radiation and inhomogeneities of the medium.

2.1.3 Scheme of the Monte Carlo method. The system consisting of Eqn (2.7) and the constitutive equation of a medium determines a random realization of the light field

$\widetilde{E}^{(i)}(\mathbf{r}, z, t)$ for some distributions of the dielectric constant $\tilde{\varepsilon}^{(i)}(\mathbf{r}, z, t)$ in the medium and of the light wave $\widetilde{E}_0^{(i)}(\mathbf{r}, t)$ in the radiation plane. The sample $\{\widetilde{E}^{(i)}(\mathbf{r}, z, t),\ i = 1, \ldots, N\}$ of light fields is arrived at by solving this system repeatedly for an ensemble of random functions $\{\tilde{\varepsilon}^{(i)}(\mathbf{r}, z, t),\ i = 1, \ldots, N\}$, which are characterized by the spectrum $\Phi_\varepsilon(\vec{\varkappa}, \omega)$, and for an ensemble of the initial conditions $\{\widetilde{E}_0^{(i)}(\mathbf{r}, t),\ i = 1, \ldots, N\}$ with the spectrum $\Phi_E(\vec{\varkappa}, \omega)$. The sample $\{\widetilde{E}^{(i)}(\mathbf{r}, z, t),\ i = 1, \ldots, N\}$ is used for statistical analysis of a random light field in a number of planes $z = \text{const}$. According to the theory of statistical modelling [61], the error in random estimates of statistical parameters $\langle\ \rangle_N$ decreases as $\sqrt{N}$.

Thus, the MCM in statistical wave optics involves the following procedures:

Formation of random fields $\widetilde{E}_0^{(i)}(\mathbf{r}, t)$ of a source and scattering screens, which simulate fluctuations of the dielectric constant in a random medium with $\tilde{\varepsilon}^{(i)}(\mathbf{r}, z, t)$ and $\tilde{\alpha}^{(i)}(\mathbf{r}, z, t)$;

obtaining realizations of the light field $\widetilde{E}^{(i)}(\mathbf{r}, z, t)$, $i = 1, \ldots, N$ by means of repeated computer solutions to the problem of propagation of the optical radiation in a nonlinear inhomogeneous medium;

and statistical processing of the ensemble $\{\widetilde{E}^{(i)}(\mathbf{r}, z, t),\ i = 1, \ldots, N\}$ of light fields obtained.

The MCM based on the PSM is widely used in studies of linear wave problems in the optics of random media. Statistical tests with the waves scattered from a phase screen have been first performed in [62], where methodical problems of the numerical simulation of the stochastic waves diffraction have been considered by the example of a thin layer of the anisotropic ionosphere. The distribution function for the intensity fluctuations of a plane wave behind a thin turbulent layer has been studied in [63] using the model of a single phase screen.

The chain PSM has been employed when studying the effect of random inhomogeneities and height gradient of the electron concentration in the ionosphere on the statistics of signals of different frequencies [64] and the frequency-selective fading of a broadband signal in the ionospheric channel [65]. The application of the PSM to studies of the wave propagation in the ionosphere has been discussed in Refs [65, 66].

The PSM is used in acoustics for investigating the effect of the internal waves on fluctuations of the acoustic signal in a submarine sound channel [67]. Fluctuations of the sound velocity are simulated by means of a random field of the internal waves produced in the form of superposition of the eigenmodes of the channel with arbitrary phases.

The MCM based on the PSM was most commonly used in the optics of turbulent atmosphere. Because fluctuations of the light wave are formed in a random field of the refractive index in the atmospheric path, the model involving many phase screens was used. In [68], the PSM was used for studying the strong intensity fluctuations of a plane wave for different parameters of the atmospheric turbulence. The model contained from twelve to twenty screens along the light propagation path, which simulated fluctuations of the refractive index with a power spatial spectrum. To determine the spectrum of the intensity fluctuations, an ensemble of ten realizations was used which was processed by applying an additional averaging in the observation plane, the latter procedure being admissible for statistically isotropic fields. In Ref. [68], the model of random continuum represented by a chain of twenty phase screens was compared with the model of a single phase screen located, according to [54], at one-half the propagation length. It was shown that a single phase screen having the same variance as the total variance of a chain of screens underestimates the variance σ_I^2 of intensity fluctuations of a plane wave approximately by 25% in a broad range of variations of the internal scale l_0 (Fig. 2).

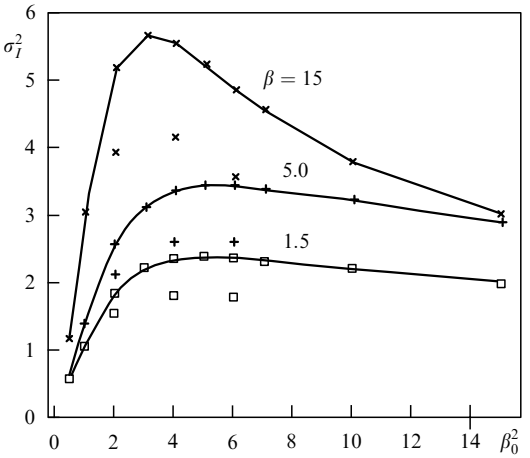

Figure 2. Comparison of dependences for the variance σ_I^2 of intensity fluctuations in a plane wave on β_0^2 obtained for the PSM consisting of 20 screens (solid lines with symbols) and of a single screen (separate symbols for $\beta_0^2 = 2, 4, 6$). Fluctuations of the medium are described by the Kolmogorov spectrum with the internal scale l_0 at $l_0/R_\text{F} = 0.6\beta$, where $R_\text{F} = \sqrt{z/k_0}$ is the Fresnel radius, the parameter β is shown near the curves, and β_0^2 is the variance of the plane wave fluctuations within the approximation of smooth perturbations [68].

A number of studies on the statistics of the light wave intensity in a turbulent atmosphere has been carried out using the procedure developed in [68]. In these papers, the variance of intensity fluctuations of the light beam was investigated [69] and the results of the numerical experiment were directly compared with natural measurements [70]. Analysis of the first five statistical intensity moments in the regions of a weak turbulence, strong focusing, and saturation of the field fluctuations showed that known asymptotic theories are valid only in the region of an extremely strong saturation of fluctuations [71]. Statistical studies of the distribution function of intensity fluctuations for the plane and spherical waves in the turbulent atmosphere have been performed in [72].

The geometrical optics approach in the PSM was put to use in [73] for studying the mean number of beams and the density of caustics upon the multibeam propagation of the waves in a random medium.

Advantages of the MCM in the wave problems of random media were discussed at length in [73], where good agreement between numerical calculations of the fourth field moment and known analytic solutions was shown.

The possibilities of the PSM employment in nonlinear problems of the laser beam propagation in the turbulent atmosphere were demonstrated in [22], where individual realizations of the light field were obtained in the case of the self-action in a random field of the refractive index. Many papers were devoted to statistical tests in the nonlinear optics of the turbulent atmosphere (see, for instance, reviews [10, 23, 75]).

The MCM was used for studying the spatial statistics of light beams in the atmosphere in the case of nonstationary thermal self-action [76] and under conditions of the wind refraction [77], as well as for determining the average statistical parameters of intense laser beams upon pulsations of the wind velocity along the atmospheric route [78, 79]. Statistical tests started from the PSM were performed for analysis of the adaptive optics systems in the atmosphere [80 – 82].

2.1.4 Phase screen model and split-step method. A chain of a finite number of scattering screens adequately reflects properties of a nonlinear continuum with randomly inhomogeneous parameters, provided the distance Δz between the screens is small compared to lengths of the characteristic change in the field along the evolution coordinate — the lengths of nonlinearity $L_{\rm nl}$, dispersion $L_{\rm dp}$, diffraction $L_{\rm df}$, and extinction α^{-1}:

$$\Delta z \ll \min\{L_{\rm nl},\, L_{\rm dp},\, L_{\rm df},\, \alpha^{-1}\}. \tag{2.14}$$

Scales $L_{\rm df}$ and $L_{\rm dp}$ of the fields for a randomly inhomogeneous wave are determined by the expressions

$$L_{\rm df} = k_0 r_{\rm c}^2\,, \quad L_{\rm dp} = \frac{\tau_{\rm c}^2}{|\partial^2 k/\partial\omega^2|}\,. \tag{2.15}$$

Under condition (2.14), the effects of nonlinearity, dispersion, diffraction, and absorption only slightly influence a change in the light field within the slab Δz. This allows one to represent the slab Δz of a random medium as a system of two screens, one of which simulates 'intrinsic' fluctuations of the dielectric constant of the medium and another simulates fluctuations induced by the field due to nonlinearity of the medium response. Behind the screens, diffraction and dispersion of the wave take place upon its propagation by the distance Δz in a linear homogeneous medium.

A continuum as a whole is represented as a chain of screens arranged in pairs. The field fluctuations caused by the screens of 'intrinsic' and induced perturbations of the medium are transformed between the screens of adjacent slabs upon diffraction and dispersion. In the absence of absorption, when the medium causes only phase perturbations of the wave, these perturbations undergo the phase-amplitude conversion between the screens and the amplitude-phase conversion on the nonlinear screens. In this case, the mutual conversion of the amplitude and phase perturbations of the wave develops under conditions of the phase stochastization by 'intrinsic' fluctuations of the randomly inhomogeneous medium.

The phase screen model of a nonlinear random medium represents in fact a physical interpretation of the split-step method (SSM), which is widely used in calculus mathematics [83]. In this method, the differential equation with a composite operator, which can be represented as a sum of simpler component operators, is replaced in each slab Δz by a chain of equations containing component operators. This permits one to use the most efficient methods for numerical solution to each of the equations in the chain. This approach applied to physics is referred to as the method of splitting by physical factors.

The SSM applied to Eqn (2.7) leads to the next chain of equations in the slab $[z_j\, z_{j+1}]$, $j = 1, \ldots, J-1$, where J is the number of slabs. The first equation describes a random perturbation of the complex phase of the field by 'intrinsic' inhomogeneities of a medium:

$$2{\rm i}k_0\,\frac{\partial\widetilde{E}_\varepsilon}{\partial z} = k_0^2\,\frac{\tilde{\varepsilon}}{\varepsilon}\,\widetilde{E}_\varepsilon - {\rm i}k_0\tilde{\alpha}\widetilde{E}_\varepsilon\,, \quad z\in[z_j z_{j+1}]\,. \tag{2.16}$$

The initial condition for this problem at $z = z_j$ is the complex amplitude at the left boundary of the slab, which is known:

$$\widetilde{E}_\varepsilon(\mathbf{r}, z_j, t) = \widetilde{E}(\mathbf{r}, z_j, t)\,.$$

The second equation describes the field distortion due to the amplitude-phase conversion during which the inhomogeneities in the intensity distribution cause nonlinear phase perturbations:

$$2{\rm i}k_0\,\frac{\partial\widetilde{E}_{\rm nl}}{\partial z} = k_0^2\,\frac{\varepsilon_{\rm nl}}{\varepsilon}\,\widetilde{E}_{\rm nl} - {\rm i}k_0(\alpha_{\rm nl}+\alpha)\,\widetilde{E}_{\rm nl}\,, \quad z\in[z_j\, z_{j+1}]\,. \tag{2.17}$$

This equation is considered simultaneously with the constitutive equation for a medium. The initial condition for $\widetilde{E}_{\rm nl}$ in the z_j-plane is the solution of the previous problem:

$$E_{\rm nl}(\mathbf{r}, z_j, t) = \widetilde{E}_\varepsilon(\mathbf{r}, z_{j+1}, t)\,.$$

The third equation describes the wave propagation in a linear regular medium of thickness Δz, during which the induced phase perturbations are transformed to amplitude perturbations:

$$2{\rm i}k_0\,\frac{\partial\widetilde{E}_{\rm w}}{\partial z} = \Delta_\perp\widetilde{E}_{\rm w} - k_0\,\frac{\partial^2 k}{\partial\omega^2}\cdot\frac{\partial^2\widetilde{E}_{\rm w}}{\partial\eta^2}\,, \quad z\in[z_j\, z_{j+1}]\,, \tag{2.18}$$

with the initial condition

$$\widetilde{E}_{\rm w}(\mathbf{r}, z_j, t) = \widetilde{E}_{\rm nl}(\mathbf{r}, z_{j+1}, t)\,.$$

The solution of the latter problem is taken as the required field at the right boundary z_{j+1} of the slab:

$$\widetilde{E}(\mathbf{r}, z_{j+1}, t) \equiv \widetilde{E}_{\rm w}(\mathbf{r}, z_{j+1}, t)\,. \tag{2.19}$$

In the next slab $[z_{j+1}\, z_{j+2}]$, the problems of scattering, nonlinear distortion, and wave propagation are again solved successively. In this case, the initial condition for the first of the problems is the one obtained previously in the z_{j+1}-plane.

The order of consideration of processes in the slab Δz is ambiguous. The above procedure results in an asymmetric scheme. Upon symmetrization, the wave propagation over a distance of $\Delta z/2$ is first considered, then inhomogeneous and nonlinear distortions of the field and then again the wave problem for a thickness of $\Delta z/2$. It is easy to see that the passage to the symmetric scheme of the problem as a whole results in changes in the first and last slabs only. At the same time, when the number of slabs is small ($J \leqslant 10$), the symmetric scheme provides a higher accuracy [75].

The idea of using the SSM in problems of wave propagation in nonlinear random media has been first suggested in a short communication [84]. The modern concept of this method and procedures for the construction of split operators for analysis of the waves in linear random media is discussed in a review article [85].

In nonlinear wave optics, the SSM has been first applied to analysis of nonstationary self-modulation of ultrashort light pulses in a nonlinear dispersive medium [86]. This

method has received wide acceptance after issuing [22] and has been further developed for the solution of many problems in nonlinear atmospheric optics [23]. At present, the split-step method constitutes a most effective procedure tailored for nonlinear wave optics and laser physics [24]. The method is used for analysis of propagation of light pulses in optical fibres [87] and beams in atmosphere [10, 75], formation of radiation in CO_2 lasers [88, 89] and high-power solid-state amplifiers [90], for studies of stimulated Raman scattering [91, 92], wave-front reversal [93], problems of adaptive optics [80 – 82], and many other problems.

2.1.5 Method of numerical experiments. The solution to the problem of field scattering by 'intrinsic' inhomogeneities of a medium (2.16) has the form

$$\widetilde{E}_\varepsilon(\mathbf{r}, z_{j+1}, t) = \widetilde{E}_\varepsilon(\mathbf{r}, z_j, t)\exp\{-\mathrm{i}\widetilde{S}_j(\mathbf{r}, t)\},$$
$$\widetilde{S}_j(\mathbf{r}, t) = \frac{1}{2}\int_{z_j}^{z_{j+1}}\left[k_0\frac{\tilde{\varepsilon}(\mathbf{r}, z', t)}{\varepsilon} - \mathrm{i}\tilde{\alpha}(\mathbf{r}, z', t)\right]\mathrm{d}z'. \quad (2.20)$$

Here, $\widetilde{S}_j$ is a random phase, which is complex in the general case. Its real part is equal to the wave-phase accumulation and the imaginary part is equal to half the optical thickness $\tilde{\theta}_j/2$ of the jth slab in an irregular medium. The perturbation of the wave phase coincides with the first-order correction in the geometrical optics approximation [40].

If the slab thickness Δz exceeds the internal, l_0, and external, L_0, perturbation scales in the medium

$$\Delta z > L_0 > l_0, \quad (2.21)$$

then the model of the dielectric constant of the medium, which is δ-correlated along the evolution coordinate z, can be applied [40]. For a statistically stationary and isotropic field $\tilde{\varepsilon}(\mathbf{r}, z, t)$, the spectrum $F_S(\vec{\varkappa}, \omega)$ of a random phase $\widetilde{S}(\mathbf{r}, t)$ on a screen takes the form [10]

$$F_S(\vec{\varkappa}, \omega) = \frac{\pi k_0^2}{2}\Delta z\Phi_\varepsilon(\vec{\varkappa}_\perp, 0, \omega), \quad (2.22)$$

where $\Phi_\varepsilon(\vec{\varkappa}_\perp, 0, \omega)$ is the spectral density of the three-dimensional nonstationary field $\tilde{\varepsilon}(\mathbf{r}, z, t)$.

For the Gaussian field $\tilde{\varepsilon}(\mathbf{r}, z, t)$, the condition of δ-correlation means the statistical independence of the phase fluctuation $\widetilde{S}$ on different screens:

$$\langle\widetilde{S}_j(\mathbf{r}, t)\,\widetilde{S}^*_{j'}(\mathbf{r}, t)\rangle = \sigma_S^2\delta_{jj'}, \quad (2.23)$$

where σ_S^2 is the variance of phase fluctuations on a screen.

In problems of atmospheric optics, the model of 'frozen' turbulence is used. In this case, the field $\widetilde{S}(\mathbf{r}, t)$ on the screen satisfies the condition

$$\widetilde{S}_j(\mathbf{r}, t) = \widetilde{S}_j(\mathbf{r} - \mathbf{v}_\perp t, 0). \quad (2.24)$$

This corresponds to the representation of the moving random medium as a sequence of screens $\widetilde{S}_j$ that are displacing with velocity $\mathbf{v}_\perp$ in the direction perpendicular to the radiation propagation.

The solution of problem (2.17) formulated on nonlinear distortions of the field has the form [23]

$$E_{\mathrm{nl}}(\mathbf{r}, z_{j+1}, t) = E_{\mathrm{nl}}(\mathbf{r}, z_j, t) \times \exp\left\{-\frac{\theta_j}{2}\right\}\exp\left\{-\mathrm{i}\varphi_{\mathrm{nl}\,j} - \frac{\theta_{\mathrm{nl}\,j}}{2}\right\}, \quad (2.25)$$

where

$$\varphi_{\mathrm{nl}\,j} = \frac{k_0}{2\varepsilon}\int_{z_j}^{z_{j+1}}\varepsilon_{\mathrm{nl}}(I)\,\mathrm{d}z, \quad \theta_{\mathrm{nl}\,j} = \int_{z_j}^{z_{j+1}}\alpha_{\mathrm{nl}}(I)\,\mathrm{d}z.$$

Expression (2.25) describes a change in the field upon scattering from a screen with perturbations of the phase $\varphi_{\mathrm{nl}\,j}$ and optical thickness $\theta_{\mathrm{nl}\,j}$ induced by the field in the slab Δz. To determine them, one should use the iteration procedure. However, in the case of a weak nonlinearity, the linearization can be performed on a screen, which corresponds to the specified field approximation in the slab Δz†:

$$\varphi_{\mathrm{nl}\,j}(\mathbf{r}, t) \simeq \frac{k_0\Delta z}{2\varepsilon}\,\varepsilon_{\mathrm{nl}}\left(|E_{\mathrm{nl}}(\mathbf{r}, z_j, t)|^2\right),$$
$$\theta_{\mathrm{nl}\,j}(\mathbf{r}, t) \simeq \frac{\Delta z}{2}\,\alpha_{\mathrm{nl}}\left(|E_{\mathrm{nl}}(\mathbf{r}, z_j, t)|^2\right). \quad (2.26)$$

In this approximation, the nonlinear length L_{nl} can be estimated, which was introduced into inequality (2.14) as a distance over which the phase accumulation φ_{nl} does not exceed, for example, $\pi/2$ and the optical thickness $\theta_{\mathrm{nl}} \leqslant 10^{-2} - 10^{-3}$:

$$L_{\mathrm{nl}} = \min\left\{\frac{\pi\varepsilon}{k_0\varepsilon_{\mathrm{nl}}}, \frac{2\times(10^{-2}-10^{-3})}{\alpha_{\mathrm{nl}}}\right\}. \quad (2.27)$$

The linear wave problem (2.18) can be solved by various numerical methods. However, the most efficient is the analysis in the spectral space of field harmonics for which the phase accumulation can be calculated exactly, whereas the difference schemes inevitably introduce the dispersion error caused by the approximation of the wave operator [94].

In the numerical analysis, the field is represented by functions of the discrete argument in the z_j-planes. For example, the complex amplitude of the light wave is given in the form

$$E(\mathbf{r}, z, t) \to E_{pqm}(z) \equiv E(x_p, y_q, z, t_m). \quad (2.28)$$

For a square grid with the spacing h:

$$x_p = ph, \quad y_q = qh, \quad p, q = 1, \ldots, P, \quad \mathcal{L} = Ph.$$

For the sampling step h_τ, we obtain

$$t_m = mh_\tau, \quad m = 1, \ldots, M, \quad \mathcal{L}_t = Mh.$$

The parameter $\mathcal{L}$ can be defined as a size of the 'computer' aperture (grid size) which is used for observation of the wave propagation, and the parameter $\mathcal{L}_t$, as the 'computer' time of the pulse observation in the accompanying coordinate system.

To obtain the solution $E_{pqm}(z_j)$ of the wave problem in the spectral space, the direct, F, and inverse, F^{-1}, Fourier transforms are used for the function of discrete argument, which are performed by means of the fast Fourier transform (FFT) algorithm. This substantially reduces computational time. The field $E_{pqm}(z_{j+1})$ is written in the form

$$E_{pqm}(z_{j+1}) = F^{-1}\left\{\exp\left[\frac{\mathrm{i}}{2k_0}(\varkappa_{p'}^2 + \varkappa_{q'}^2 + \varkappa_{q'}^2\omega_{m'}^2)\Delta z\right]F\left[E_{pqm}(z_j)\right]\right\}, \quad (2.29)$$

†The specified field approximation in the slab Δz imposes a substantially weaker limitation than this approximation but applied to the total propagation length z_J.

where

$$\omega_{m'} = \left(k_0 \frac{\partial^2 k}{\partial \omega^2}\right)^{1/2} \frac{2\pi}{\mathcal{L}_t} m', \quad \varkappa_{p'} = \frac{2\pi}{\mathcal{L}} p', \quad \varkappa_{q'} = \frac{2\pi}{\mathcal{L}} q'$$

are the frequencies of the space–time spectrum and $p', q' = 1, \ldots, P$; $m' = 1, \ldots, M$ are the serial numbers of harmonics.

Studies of the wave field in a linear random medium by various numerical methods showed [74] that the splitting procedure, i.e. the use of the PSM, reduces computational time approximately by 30% as compared to the direct solution of stochastic parabolic equation (2.7) at $\alpha_{\rm nl}, \varepsilon_{\rm nl} = 0$. The use of the FFT algorithm therewith increases the efficiency of the SSM especially in the case of intense fluctuations.

Detailed analysis of the efficiency of different numerical methods by the example of the problem of a soliton in a regular medium with cubic nonlinearity has been performed in [24]. It has been found that the SSM in conjunction with the FFT algorithm requires a substantially smaller number of sampling intervals Δz and h in comparison with difference schemes for the same accuracy of conserving the integrals of motion. For this reason, the computational time in the SSM is reduced by a factor of ten and more as compared to that in finite difference methods.

In Ref. [95], an algorithm of the wide-angle SSM has been developed for the modified parabolic equation that is valid in the case of a considerable change in the direction of the wave vector in media with intense large-scale fluctuations of parameters. This algorithm is intended for studies of submarine acoustic channels.

2.1.6 Adequacy of numerical analysis. The representation of fields on a discrete grid in a numerical analysis is equivalent to the long-wavelength approximation of the fields in the plane $z = \text{const}$ [94]. The grid spacing h bounds the minimum scale of the field below, the latter being reproduced in the numerical experiment:

$$\min\{r_c, l_\varepsilon\} = 2h\,, \qquad \tau_{\rm c} = 2h_\tau\,. \tag{2.30}$$

The close condition was formulated for the spacing h of the grid applied to the phase screen of the atmospheric turbulence [65]:

$$h < \frac{l_0}{3}\,,$$

where l_0 is the internal scale of the turbulence.

It follows from (2.30) that the highest frequency of the spatial spectrum of the field with a discrete argument, which is called the Nyquist frequency $\varkappa_{\rm N}$ of the grid, equals

$$\varkappa_{\rm N} = \frac{\pi}{h}\,. \tag{2.31}$$

The lowest frequency $\varkappa_1$ of the spatial spectrum for the field on the grid is inversely proportional to the size of its 'computer' aperture:

$$\varkappa_1 = \frac{2\pi}{\mathcal{L}}\,. \tag{2.32}$$

According to (2.28), the relative width of the spectral range for spatial frequencies on the grid is

$$\frac{\varkappa_{\rm N}}{\varkappa_1} = P\,,$$

and that of the time range is equal to

$$\frac{\omega_M}{\omega_1} = M\,. \tag{2.33}$$

This range should contain the time-space spectrum of all the fields reproduced in the numerical experiment. Otherwise, the errors appear in the spectral space. When using the discrete Fourier transform, these errors are related to the frequency aliasing, which results in the appearance of spurious harmonics in the field spectrum [96, 97].

When optical waves are propagating through a random medium under conditions of intense fluctuations, spatial harmonics of the light field E can appear with the frequency $\varkappa_E$ that is higher than the upper bound $\varkappa_\varepsilon$ of the spectrum Φ_ε of 'intrinsic' inhomogeneities of the medium. Upon nonlinear optical interaction, the spatial spectra of fields E and $\varepsilon_{\rm nl}$ are enriched and the maximum frequency $\max \varkappa_E$ in the spectrum of the field Φ_E increases. For this reason, the condition [22, 97]

$$\max\{\varkappa_E(z=0)\,,\ \varkappa_\varepsilon\} < \varkappa_{\rm N}\,. \tag{2.34}$$

is imposed on the upper bound of the spectrum $\Phi_E(z=0)$ of the incident wave and the spectrum Φ_ε of 'intrinsic' inhomogeneities of the medium. As a result, a 'buffer' zone is formed in the spectral space, which is intended for filling by the high-frequency harmonics of fields E and $\varepsilon_{\rm nl}$; the latter can appear in the case of intense fluctuations and nonlinear optical interactions. The spectra of fields E and $\varepsilon_{\rm nl}$ are usually unbounded, and in practice it is sufficient to control that the energy of the highest harmonics of the light field $E(\varkappa_P, \varkappa_P, \omega_M)$ on the grid would be small for any z. For example,

$$\left|E(\varkappa_P, \varkappa_P, \omega_M)\right|^2 \leqslant 10^{-(2-4)} \max_{p', q', m'} \left\{\left|E(\varkappa_{p'}, \varkappa_{q'}, \omega_{m'})\right|^2\right\}. \tag{2.35}$$

A specific analysis of the effect of variance of the screen phase fluctuations on the parameters of the calculating grid was performed in [65, 68]. For a screen with a Gaussian phase spectrum, the following estimate of the grid spacing h is obtained from condition (2.31) [65]:

$$h < \frac{\pi l_S}{\sqrt{2}\,\sigma_S}\,, \tag{2.36}$$

where σ_S^2 and l_S are the variance and the coherence scale of phase fluctuations on a screen. In [68], based on asymptotic estimates of the spectrum of strong fluctuations of the plane-wave intensity in the turbulent atmosphere, the expression

$$P = 2(\sigma_I^2)^{2/\gamma} 10^{1/\gamma+2} \left[\frac{1+\gamma/2}{2\gamma\Gamma(1+\gamma/2)\cos(\pi\gamma/4)}\right]^{2/\gamma} \tag{2.37}$$

was obtained for a necessary number P of the grid points, where σ_I^2 is the variance of intensity fluctuations and γ is the exponent in the power spectrum of fluctuations of the dielectric constant in a medium. Under condition (2.37), the amplitudes of harmonics at the lower and upper bounds of the intensity range on the grid do not exceed 1% of the amplitude of fundamental spectral components. According to (2.37),

for example, for the Kolmogorov spectrum of the atmospheric turbulence ($\gamma = 5/3$) [40], one can achieve the variance of intensity fluctuations $\sigma_I^2 \simeq 15$ on the grid phase screen containing 512×512 points and $\sigma_I^2 \simeq 25$ on the screen containing 1024×1024 points.

The 'computer' apertures $\mathcal{L}$ and $\mathcal{L}_t$ are, as a rule, far shorter than the real region, where the light beam propagates, and than the duration of pulse observation, respectively. However, the effect of the 'computer' aperture is small provided the field at its boundaries is close to zero for any z:

$$\left|E(\mathcal{L},\mathcal{L},\mathcal{L}_t,z)\right|^2 \leqslant 10^{-(2-4)} \max_{p,q,m}\left\{\left|E_{p,q,m}(z)\right|^2\right\}. \qquad (2.38)$$

Because the beam and the pulse are spreading out during their propagation due to diffraction, dispersion, and nonlinear effects, the field amplitude at the aperture boundary increases. To eliminate possible errors, which can arise in this case, the size of the 'computer' aperture is chosen by taking into account the ensuing increase in the beam radius $a(z)$ and in the pulse duration $t_p(z)$. For example, one obtains [97]

$$\mathcal{L} \geqslant \beta a_0\,, \qquad \mathcal{L}_t \geqslant \beta \frac{t_p}{2}\,. \qquad (2.39)$$

The value of the numerical coefficient β determines the size of the 'buffer' zone in the space of variables x, y, t, which is necessary for delocalization of radiation during its propagation. Usually, $\beta \simeq 6-10$.

The numerical solution of the wave problem in the spectral space (2.29) imposes the periodicity of the fields with a period equal to the size of the 'computer' aperture. Under condition (2.39), such a periodicity does not introduce a noticeable error into analysis of limited beams and moments. In the case of plane waves, the periodicity results in additional continuity conditions for the amplitude and phase of the light field at the aperture boundaries, thereby eliminating the appearance of purely computational diffraction on these boundaries [68]. However, a random field in the vicinity of the opposite boundaries of the 'computer' aperture shows a false correlation, and these regions should be excluded during statistical processing. The relative sizes of these regions are small provided the aperture diameter $\mathcal{L}$ exceeds the transverse shift of the spectral components appearing in the chain of phase screens. For a one-scale screen, this condition yields the following estimate [65]:

$$\mathcal{L} > \frac{\sqrt{2}\,\sigma_S z}{k_0 l_S}\,. \qquad (2.40)$$

Along with control over the filling of buffer zones, the important factor characterizing the reliability of results of the numerical experiment is the conservation of integrals of motion inherent in the problem [24]. In a medium without losses, the radiation energy W does not change with z:

$$\frac{\mathrm{d}W}{\mathrm{d}z} = 0\,, \quad W = \frac{cn_0\varepsilon_0}{2}\int_{\mathcal{L}} EE^*\,\mathrm{d}^2r\,\mathrm{d}\eta\,. \qquad (2.41)$$

In isotropic media, the 'transverse momentum' p of the wave is also the integral of motion:

$$p = \frac{\mathrm{i}n_0\varepsilon_0}{k_0}\int_{\mathcal{L}} (E\nabla_{\perp\eta}E^* - E^*\nabla_{\perp\eta}E)\,\mathrm{d}^2r\,\mathrm{d}\eta\,. \qquad (2.42)$$

The value of p determines the beam 'trend' in a plane perpendicular to the coordinate z, the pulse 'drift' in the moving coordinate system. The trend of a partially coherent beam results from the presence of a random component of the inclination of the beam wave vector in the plane $z = 0$, while the pulse drift is caused by a random frequency deviation upon phase modulation.

For large values of p, the region of the radiation localization is displaced over the 'computer' aperture in the initial plane $z = 0$, which can result in an increase in the field at the aperture boundary. Since this violates condition (2.39), the realizations of the random field $\widetilde{E}_0(\mathbf{r},t)$ with the 'momentum' p exceeding some threshold value are discarded.

In the absence of absorption in media with Kerr nonlinearity, the Hamiltonian H of the system is also conserved:

$$H = \int_{\mathcal{L}} \left(\nabla_{\perp\eta}E\nabla_{\perp\eta}E^* - \varphi(|E|^2)\right)\mathrm{d}^2r\,\mathrm{d}\eta\,, \qquad (2.43)$$

where

$$\varphi(|E|^2) = \frac{k_0^2}{\varepsilon}\left(\int_0^{|E|^2} \varepsilon_{\mathrm{nl}}(\xi)\,\mathrm{d}\xi + \tilde{\varepsilon}|E|^2\right)$$

is the function of $|E|^2$.

2.2 Formation of random fields

2.2.1 Field models. Realizations of the partially coherent radiation $\widetilde{E}_0^{(i)}(\mathbf{r},t)$ or random phase $\widetilde{S}^{(i)}(\mathbf{r},t)$ on a screen are usually obtained by means of the statistical model of the field being formed. In the case of optical radiation, the model of 'noise burst' in the form of a narrowband Gaussian noise is most often used [1]. In this model, the complex amplitude of a pulse is represented in the form

$$\widetilde{E}_0(t) = A_0(t)\tilde{\gamma}(t)\,, \quad \tilde{\gamma}(t) = \tilde{c}(t) + \mathrm{i}\tilde{d}(t)\,. \qquad (2.44)$$

The quadrature components $\tilde{c}(t)$ and $\tilde{d}(t)$ are statistically independent, they have the normal distribution $w(c)$ and a Gaussian autocorrelation function $\Gamma(\tau)$:

$$\begin{aligned} &\langle\tilde{c}(t)\rangle = \langle\tilde{d}(t)\rangle = 0\,, \quad \langle\tilde{c}(t)\,\tilde{d}(t)\rangle = 0\,,\\ &w(\tilde{c}) = \sqrt{\pi}\exp\{-\tilde{c}^2\}\,,\\ &\Gamma(\tau) = \langle\tilde{c}(t)\,\tilde{c}(t-\tau)\rangle = \frac{1}{2}\exp\left\{-\frac{\tau^2}{\tau_{c0}^2}\right\}, \end{aligned} \qquad (2.45)$$

where τ_{c0} is the coherence time for a random substructure of the input pulse.

For a noise burst, whose phase modulation is on average zero and the shape is Gaussian, the envelope $A_0(t)$ is

$$A_0(t) = A_0\exp\left\{-\frac{t^2}{2t_p^2}\right\}, \qquad (2.46)$$

where t_p is the pulse duration. In this case, $t_p > \tau_{c0} \gg 2\pi/\omega_0$.

The correlation function of radiation $\Gamma(t,\tau) = \langle\widetilde{E}_0(t-\tau/2)\,E_0^*(t+\tau/2)\rangle$ can be represented in the form

$$\begin{aligned} &\Gamma(t,\tau) = A_0^2\exp\left\{-\frac{t^2}{t_p^2}\right\}\exp\left\{-\frac{\tau^2}{\theta_{c0}^2}\right\},\\ &\theta_{c0}^{-2} = (2t_p)^{-2} + \tau_{c0}^{-2} \end{aligned} \qquad (2.47)$$

or

$$\Gamma(t,\tau) = A_0^2\exp\left\{-\frac{t^2+N\tau^2}{t_p^2}\right\},$$

where $N = 1/4 + t_p/\tau_{c0}^2$ is the parameter characterizing the number of inhomogeneities of the complex amplitude of the field per pulse duration t_p.

The Gaussian pulse with an additive noise is determined by the expression

$$\widetilde{A}_0(t) = \frac{A_0}{(1+m^2)^{1/2}} \exp\left\{-\frac{t^2}{2t_p^2}\right\}\left(1 + m\tilde{\gamma}(t)\right). \qquad (2.48)$$

In the case of a random phase modulation, it follows that

$$\widetilde{A}_0(t) = A_0 \exp\left\{-\frac{t^2}{2t_p^2}\right\} \exp\left\{i\tilde{\varphi}(t)\right\}, \qquad (2.49)$$

where $\tilde{\varphi}(t)$ is uniformly distributed over the interval $[0, 2\pi]$.

In the case of a partially coherent light beam, which has on average a plane wave front and a Gaussian profile, the field can be represented in the form

$$\widetilde{E}_0(r) = A_0 \exp\left\{-\frac{r^2}{2a_0^2}\right\}\left(\tilde{c}(r) + i\tilde{d}(r)\right). \qquad (2.50)$$

This corresponds to a statistically quasi-isotropic field whose spatial correlation function equals

$$\Gamma(r,\rho) = A_0^2 \exp\left\{-\frac{r^2}{a_0^2}\right\} \exp\left\{-\frac{\rho^2}{r_{c0}^2}\right\}, \qquad (2.51)$$

where r_{c0} is the coherence radius.

The field of a Gaussian beam scattered from a phase screen has the form

$$\widetilde{E}_0(r) = E_0 \exp\left\{-\frac{r^2}{2a_0^2}\right\} \exp\left\{i\widetilde{S}(r)\right\}, \qquad (2.52)$$

where $\widetilde{S}(r)$ is the random phase with a known spatial spectrum $F_S(\varkappa)$ or correlation function $\Gamma_S(\rho)$.

There are different models of the atmospheric turbulence, which are based on the Kolmogorov – Obukhov law of two-thirds [98]. One of the most popular models is the Kármán model, in which the spectrum of spatial fluctuations of the dielectric constant is described by the Kolmogorov power law within the inertial interval $l_0 < r < L_0$ and it is saturated at lower frequencies $\varkappa < \varkappa_0 = 2\pi/L_0$ [40, 99]:

$$\Phi_\varepsilon(\varkappa_\perp, \varkappa_z) = 0.033 C_\varepsilon^2 (\varkappa_0^2 + \varkappa_\perp^2 + \varkappa_z^2)^{-11/6}, \qquad (2.53)$$

where C_ε^2 is the structural constant, and L_0 is the external scale of the turbulence. According to (2.22), the two-dimensional phase spectrum in the slab Δz has the form

$$F_S(\varkappa_\perp) = \frac{5\sigma_S^2}{6\pi} \varkappa_0^{5/3} (\varkappa_0^2 + \varkappa_\perp^2)^{-11/6}. \qquad (2.54)$$

The correlation phase function [100]

$$\Gamma_S(\rho) = \frac{2^{1/6}}{\Gamma(5/6)} \sigma_S^2 (\varkappa_0\rho)^{5/6} K_{5/6}(\varkappa_0\rho) \qquad (2.55)$$

is expressed in terms of the Macdonald function $K_{5/6}(\varkappa_0\rho)$ and gamma function $\Gamma(5/6)$. The variance σ_S^2 of phase fluctuations equals [99]

$$\sigma_S^2 = 0.195 C_\varepsilon^2 k_0^2 \varkappa_0^{-5/3} \Delta z. \qquad (2.56)$$

2.2.2 Formation methods. Realizations of random fields $\widetilde{E}^{(i)}$ and $\widetilde{S}^{(i)}$ are formed as functions of a discrete argument of the type (2.28). The fields $\widetilde{E}$ and $\widetilde{S}$ with the specified correlation function or spectrum are obtained by means of the transformation of the δ-correlated random field $\tilde{\eta}_{pqm}$, which is generated at the grid nodes:

$$\langle \tilde{\eta}_{pqm} \tilde{\eta}_{p'q'm'} \rangle = \delta_{pp'} \delta_{qq'} \delta_{mm'}. \qquad (2.57)$$

In the linear transformation method [61, 101], $\widetilde{E}_{pqm}$ is calculated from $\tilde{\eta}_{pqm}$ with the help of a matrix that determines the correlation dependence of the required field. In the case of high-dimensionality problems ($PQM > 10^5$), this method requires very long computation time.

In the spectral method [101, 102], the complex field is represented as a sum of the Fourier harmonics with random amplitudes and phases. Thus, the field $\tilde{\gamma}_m$ for (2.44) is written in the form

$$\tilde{\gamma}_m = \frac{1}{\sqrt{M}} \sum_{k=0}^{M-1} a_k (\tilde{\xi}_k + i\tilde{\eta}_k) \exp\left\{i\frac{2\pi}{M} mk\right\}, \quad m = 0, 1, \ldots, M-1, \qquad (2.58)$$

$$\langle \tilde{\xi}_k \tilde{\eta}_{k'} \rangle = 0, \quad \langle \tilde{\xi}_k \tilde{\xi}_{k'} \rangle = \langle \tilde{\eta}_k \tilde{\eta}_{k'} \rangle = \frac{1}{2} \delta_{kk'}.$$

The weight factors a_k of harmonics are determined by the correlation function Γ_l of quadrature components $\tilde{c}_m$ and $\tilde{d}_m$ of the field required:

$$a_k^2 = \sum_{l=0}^{M-1} \Gamma_l \cos\left(\frac{2\pi}{M} lk\right). \qquad (2.59)$$

The canonical expansion method [61], where some coordinate functions are summarized with random coefficients, is algorithmically close to the spectral method. These functions can be the eigenfunctions of the integral equation whose kernel is the correlation function Γ_l of the required field.

The spectral method with the use of a fast Fourier transform algorithm is characterized by a high computational efficiency. However, because of features of the Fourier transform on a discrete grid [103], the correlation function Γ_l is periodic [62]: $\Gamma_l = \Gamma_{M-l}$. As a result, strictly speaking, one can use the fields γ_m containing $M/2$ values on a one-dimensional grid containing M nodes, and on a two-dimensional grid containing PQ nodes — the field in one fourth of the grid: $p = 0, \ldots, P/2-1$; $q = 0, \ldots, Q/2-1$. This should be taken into account when forming the buffer zones (2.39) at the 'computer' aperture boundaries. If the coherence scale of the field is far smaller than the aperture size ($\beta \gg 1$), a false phase correlation is insignificant [62]. To reduce the systematic error in the method due to the discrete representation of the fields, it was suggested [104] to introduce the weight factor for correcting the variance of phase fluctuations on a screen.

Within the spectral approach, a random field is formed simultaneously at all the nodes of a grid. For this reason, nonstationary problems of the atmospheric optics, in which models of the 'frozen' turbulence are used, require a large memory capacity for a storage of phase screens $\widetilde{S}_{pqm}$ travelling with the wind flow. These difficulties can be overcome by the moving summation method [61, 100, 101], in which the required phase $\widetilde{S}_{pqm}$ is calculated by the weighted summation of the δ-correlated

field $\tilde{\eta}_{pqm}$ displaced over the grid. Thus, the stationary screen $\widetilde{S}_{pq}$ on a rectangular grid is determined by the expression

$$\widetilde{S}_{pq} = \sum_{l=-p_k}^{p_k} \sum_{j=-q_k}^{q_k} C_{lj} \tilde{\eta}_{p+l\, q+j} ,$$
$$p = p_k + 1, \ldots, P - p_k ; \quad q = q_k + 1, \ldots, Q - q_k . \quad (2.60)$$

The weight coefficients C_{lj} are calculated from the spectral density $F_S(\varkappa_x, \varkappa_y)$ of the modulated field $\widetilde{S}(x, y)$:

$$C_{lj} = \frac{1}{\pi h} \int_0^{\varkappa_N} F_S^{1/2}(\varkappa_x, \varkappa_y) \cos(lh\varkappa_x) \cos(jh\varkappa_y)\, \mathrm{d}\varkappa_x\, \mathrm{d}\varkappa_y ,$$
$$l = -p_k, \ldots, p_k , \quad j = -q_k, \ldots, q_k . \quad (2.61)$$

The systematic error of the method decreases with increasing the number N of terms in (2.60) for a field with the specified scale r_c on a grid with the spacing h. In the general case, one finds

$$N = \alpha \frac{r_c}{h} , \quad N = \max\{2p_k + 1,\ 2q_k + 1\} . \quad (2.62)$$

The error parameter α is equal to the ratio of the maximum displacement Nh of the elements of the δ-correlated field $\tilde{\eta}_{pq}$ to the scale r_c. For the fields with Gaussian or Kármán spectrum (2.53), the satisfactory accuracy is achieved for $\alpha \geqslant 3$ [100].

2.2.3 Atmospheric turbulence. The size of inhomogeneities in the surface boundary layer of the turbulent atmosphere varies from an internal scale l_0 of 0.5 – 10 mm to an external scale L_0 of the order of the path height [105]. Therefore, the range of the spatial scale of fluctuations is $L_0/l_0 \sim 10^4 - 10^5$. Despite the fact that the spectral density of (2.53) decreases proportionally to $\varkappa^{-11/3}$, both the low-frequency and high-frequency harmonics of the spatial spectrum affect fluctuations of the light field in the atmosphere. Phase screens of the atmospheric turbulence are usually constructed with the spectral method [22, 62, 65, 68] and less commonly, by the moving summation method [100]. The possibility of applying the other methods are briefly discussed in [104].

In a random field formed on a grid, the minimum scale l_0 is determined by the Nyquist frequency $\varkappa_N$ of the grid and, according to estimates [106], is $l_0 = (1.5-2)h$. The maximum scale of inhomogeneities in the fields obtained by the spectral method or moving summation method is close to the size of the 'computer' aperture $\mathcal{L}$. Thus, according to (2.30) and (2.39), the external, L_0, and internal, l_0, scales of turbulence, the beam radius a_0, and parameters $\mathcal{L}$ and h of the grid in the numerical experiment satisfy a chain of inequalities

$$\mathcal{L} > L_0 \gg a_0 \gg l_0 > h . \quad (2.63)$$

Formation of the two-dimensional field $\widetilde{S}$ with a random phase, in which the relative change in the inhomogeneity size achieves several orders of magnitude, requires excessively long computing time. In numerical experiments, the external scale L_0 of the order of $(8-10)a_0$ is usually chosen. This leads to underestimation of the contribution from large-scale fluctuations that cause lowest-order optical aberrations, which are manifested in a random walk and focusing of the light beam in the atmosphere. Such a systematic error arises because the Fourier harmonics, which form the basis set in the spectral method, strongly differ from optical aberration fluctuations in the atmosphere,

In [107], it was suggested to use the Zernike polynomials $Z_i(\rho, \theta)$, which are commonly applied in describing aberrations in optical systems, as a basis set for forming phase fluctuations in the turbulent atmosphere. In a modal representation, the screen phase $\widetilde{S}$ on a circular aperture with radius R has the form

$$\widetilde{S}(\rho, \theta) = \sum_{i=2}^{\infty} \tilde{\alpha}_i Z_i(\rho, \theta) , \quad \rho = \frac{r}{R} . \quad (2.64)$$

Expansion coefficients $\tilde{\alpha}_i$ are the random numbers possessing the normal distribution with $\langle \tilde{\alpha}_i \rangle = 0$.

For the Kolmogorov turbulence model of the atmosphere described by (2.54) at $\varkappa_0 = 0$, the variance of these coefficients is [108]:

$$\langle \tilde{\alpha}_i^2 \rangle = \alpha_i^2 \left(\frac{2R}{r_0} \right)^{5/3} , \quad (2.65)$$

where $r_0 = 1.68(C_n^2 k_0 \Delta z)^{-3/5}$ is the coherence radius of Fried [109] and $C_n^2 = 4C_\varepsilon^2$. Weight factors α_i^2 rapidly decrease with increasing serial number of the expansion term. For the first-order aberrations describing the tilt of the wave front, $\alpha_2^2 = \alpha_3^2 = 4.49 \times 10^{-1}$. For the second-order aberrations corresponding to defocusing and astigmatism, $\alpha_4^2 = \alpha_5^2 = \alpha_6^2 = 2.32 \times 10^{-2}$, and for coma, $\alpha_7^2 = \ldots = \alpha_{10}^2 = 6.19 \times 10^{-3}$ [108]. For the Kármán model (2.53) at $\varkappa_0 \neq 0$, the decrease in factors α_i slows down, the effect being stronger with decreasing ratio of the external scale L_0 to the aperture radius R. In this case, always $L_0/R > 1$.

The choice of the aperture radius R in modal representation (2.64) is ambiguous. Some approaches to the solution of this problem are discussed in [110, 111].

There is a correlation between weight factors $\tilde{\alpha}_i$ in the expansion of atmospheric phase fluctuations over Zernike polynomials (2.64). Thus, the correlation coefficients for tilt and coma are $\langle \tilde{\alpha}_2 \tilde{\alpha}_8 \rangle = \langle \tilde{\alpha}_3 \tilde{\alpha}_7 \rangle = 1.42 \times 10^{-2}$ [108].

The presence of correlation between $\tilde{\alpha}_i$ substantially complicates the procedure of generating a random phase field in the basis of Zernike polynomials. The orthonormalized basis for the atmospheric turbulence is formed by the Karhunen – Loeve – Obukhov (KLO) functions, which are the eigenfunctions of the like integral equation. The KLO functions were numerically calculated from this equation and were shown to form the optimum basis for the phase expansion in the turbulent atmosphere [108]. The mean-square phase deviation in this expansion shows a minimum as compared to other expansions containing the same number of terms. In [112], the method was developed that entered into the numerical generation of a random phase field in the atmosphere by means of the matrix transforming the Zernike basis to the KLO basis. In [113, 114], analytic expressions were obtained for KLO functions in the form of expansions in terms of the Bessel functions and the error of this representation was estimated for a finite number of terms.

The modal approach permits the adequate reproduction of large-scale phase fluctuations, whereas the spectral one reproduces small-scale fluctuations. This is confirmed by the results of statistical tests of phase screen fields obtained by the modal method for a finite number of expansion terms ($\max i = J$) and by the spectral method on a grid containing $P \times Q$ nodes (Fig. 3) [115]. To analyze a random field $\widetilde{S}(\rho)$

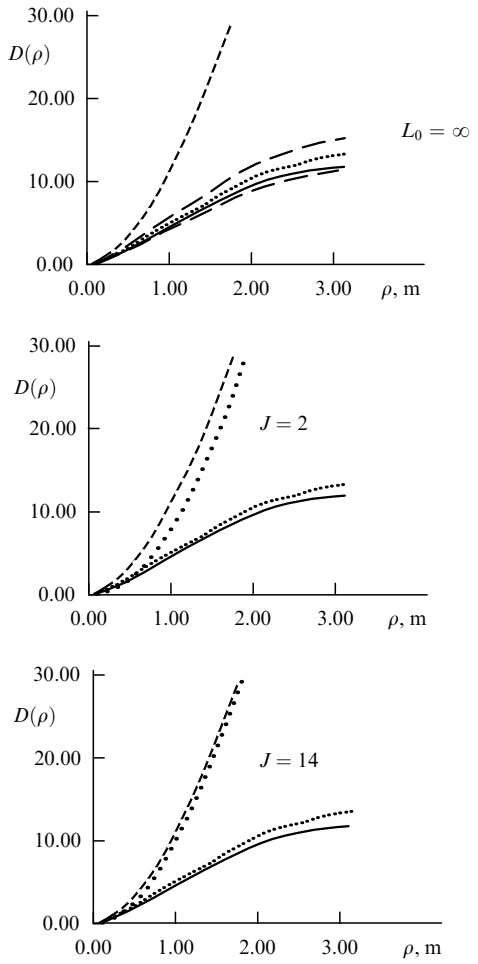

Figure 3. Structural function $D_S(\rho)$ of phase fluctuations on a screen calculated by the MCM for a random field $\tilde{S}(\rho)$ obtained by the modal method for $J = 14$ (rare points) and by the spectral method for $P \times Q = 128 \times 128$ (dense points) at the aperture $\mathcal{L} = R = 6.4$ m. The number of realizations $N = 10^2$: the Kolmogorov turbulence model with $L_0 = \infty$, the confidence interval (long dashes), D_5 expected on a grid (solid curve), analytical dependence (dashed curve).

with a broad range of spatial scales, the structural function $D_S(\rho)$ was used [40]:

$$D_S(\rho) = \left\langle \left(\widetilde{S}(\rho) - \widetilde{S}(0)\right)^2 \right\rangle . \tag{2.66}$$

The function $D_S(\rho)$ obtained by the spectral method for the Kolmogorov turbulence model of the atmosphere is qualitatively different from the analytic dependence. In the case of the modal method, D_S is close to the analytic dependence when the number of expansion terms is comparatively small.

For the Kármán model with the external scale $L_0 \leqslant \mathcal{L}$, the spectral and modal methods yield functions $D_S(\rho)$ that are close to the analytic dependence. However, for small ρ, the error in $D_S(\rho)$ within the modal approximation is substantially greater than that in the spectral method.

To obtain the screens simulating both the large- and small-scale phase fluctuations, the algorithm of embedded grids was suggested [116]. A screen formed by the spectral method (2.58) is covered by a low-frequency (large-mesh) grid with a spacing equal to the 'computer' aperture $\mathcal{L}$ of the screen. The resulting phase at the aperture $\mathcal{L}$ is a sum of phases of the initial and low-frequency grids. In [117], large-scale inhomogeneities are produced on a screen by introducing a number of subharmonics whose spatial frequencies are obtained by dividing the interval $(0, \varkappa_1)$ repeatedly, where $\varkappa_1 = 2\pi/\mathcal{L}$ is the lowest frequency of the initial grid screen (2.32). These approaches were modified later in [118].

2.2.4 Imitative simulation of a multimode laser beam. Models based on a specified correlation function of the type (2.47), (2.51) permit the construction of statistically isotropic and stationary random fields. However, as experiments have shown [1], the spatial statistics of laser beams upon generation of several transverse modes proves to be far more complicated. Realizations of a multimode laser beam can be obtained by the technique of imitative simulation in which a random field is formed as a superposition of the resonator modes.

By assuming the transverse modes to be statistically independent and degenerate in frequency, a field of the optical resonator can be represented in the form [119]

$$\widetilde{E}_0(\rho, \theta) = \sum_{l,p} a_{lp}\, \widetilde{F}_{lp}(\rho, \theta) \cos \tilde{\varphi}_{lp} , \tag{2.67}$$

where l and p are the azimuthal and radial indices of a mode; $\widetilde{F}_{lp}(\rho, \theta)$ is the amplitude of a random field distribution in the mode; a_{lp} are the weight coefficients depending on diffractive losses of the resonator, and $\tilde{\varphi}_{lp}$ is a random phase of the generation initiation.

For a resonator with circular mirrors, one obtains

$$\widetilde{F}_{lp}(\rho, \theta) = E_0 f_{lp}(\rho) \cos(l\theta + \widetilde{\psi}_{lp}) , \tag{2.68}$$

where $\tilde{\psi}_{lp}$ is the phase of a random orientation of a mode over azimuth θ. Phases $\tilde{\varphi}_{lp}$ and $\tilde{\psi}_{lp}$ are uniformly distributed from $-\pi$ to π.

In the case of statistically independent modes, one has

$$\langle \tilde{\varphi}_{lp} \tilde{\varphi}_{l'p'} \rangle = \langle \tilde{\psi}_{lp} \tilde{\psi}_{l'p'} \rangle = \frac{\pi^2}{3}\, \delta_{ll'} \delta_{pp'} . \tag{2.69}$$

Functions $f_{lp}(\rho)$ and coefficients a_{lp} are the solutions of the eigenvalue problem for an empty optical resonator. The analytic solution to this problem was obtained in the case of spherical mirrors for the Fresnel number $N_F \to \infty$, where $N_F = a_m^2/\lambda b$, here a_m is the mirror radius, and b is the distance between mirrors [120]. For $N_F > 1$, these solutions are close to the exact ones and can be used to obtain field realizations.

As the azimuthal and radial indices l and p increase, so do the diffraction losses of the modes, especially for small values of N_F. This allows one to estimate the number of significant terms M in (2.67). Thus, taking into account all the modes whose losses do not exceed 5%, the number $M = 24$ for $N_F = 2$ and $M = 116$ for $N_F = 6$.

To obtain the individual realization of multimode radiation $\widetilde{E}_0^{(i)}(\rho, \theta)$, a set of random phases $\tilde{\varphi}_{lp}^{(i)}$ and $\tilde{\psi}_{lp}^{(i)}$ is generated for the serial numbers of all modes forming a beam with a specified number N_F inside the resonator. Then, the complex amplitude of the field $\widetilde{E}_0^{(i)}(\rho, \theta)$ is calculated at the beam cross section from (2.67) and (2.68). The intensity distribution in the realization thus obtained represents speckles, which are characteristic for radiation from a multimode laser (Fig. 4a). Here, the neck radius w of the fundamental mode with $p = 0$

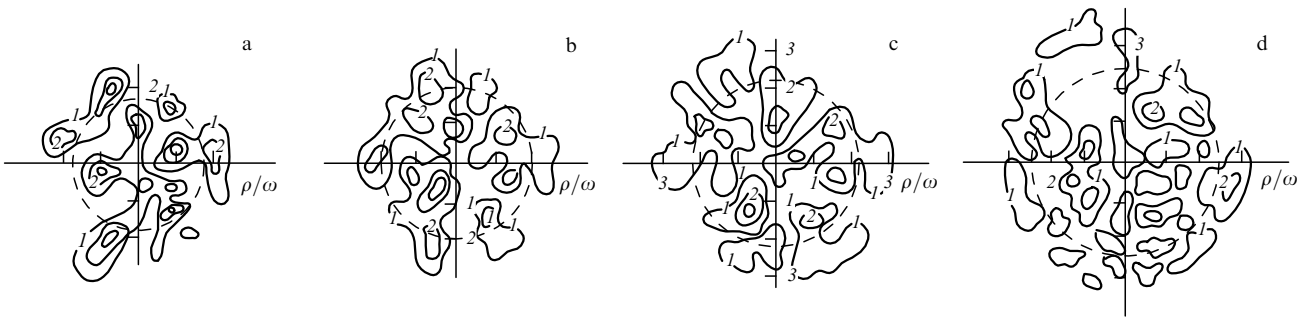

Figure 4. Isophotes in a beam cross section for a random realization of the field of a multimode laser with a symmetric spherical resonator for the Fresnel number $N_F = 2$ [119, 161]: (a) at the output aperture; (b) upon propagation in a linear medium at the distance $z = 0.25k_0w^2$; (c) and (d) upon nonstationary thermal self-action at the points in time $t = (1/3)t_p$ and $t = t_p$, respectively. The isophotes correspond to intensities (*1*) $I = 0.3I_{eq}$, (*2*) $1.3I_{eq}$, and (*3*) $2.3I_{eq}$, where I_{eq} is the peak intensity of the equivalent Gaussian beam whose power and radius coincide with corresponding average values for multimode laser radiation. The broken lines show regions restricted by radius $\langle a_{eff}\rangle_N$.

and $l = 0$ was chosen as a scale for the transverse coordinate ρ. For a confocal resonator, $w = (\lambda b/\pi)^{1/2}$.

The light field at the beam cross section is statistically inhomogeneous. The coherence scale r_c, found from the spatial coherence function of the field $\Gamma_E(\boldsymbol{\rho}_0 - \boldsymbol{\rho}/2, \boldsymbol{\rho}_0 + \boldsymbol{\rho}/2)$, substantially depends on the distance ρ_0 to 'the centre of gravity' of the separated points and on the mutual orientation of vectors $\boldsymbol{\rho}_0$ and $\boldsymbol{\rho}$.

The field coherence improves at the beam periphery, most notably for the longitudinal scale $r_{c||}$ determined for collinear vectors $\boldsymbol{\rho}_0$ and $\boldsymbol{\rho}$.

The results of statistical processing of an ensemble containing from 200 to 400 realizations of $\tilde{E}_0^{(i)}(\rho, \theta)$ showed [119] that as the Fresnel number N_F increases, the region of spatial localization of radiation expands, while the coherence radius r_c of a beam diminishes. Therefore, the coherence coefficient of the beam $c = r_c/\langle a_{eff}\rangle$ decreases (here $\langle a_{eff}\rangle$ is the mean value of the effective radius whose square is defined as the second moment of the intensity divided by the beam power). However, the production $r_c(0)\langle a_{eff}\rangle$, which determines the diffraction divergence of a partially coherent beam, is independent of N_F. The results of statistical studies on the imitative model of a multimode beam are in good agreement with experimental data and do not contradict to analytic estimates [1].

2.3 Convergence of the method

2.3.1 Errors in the phase screen method. A study of the convergence involves analysis of the effect of sampling interval choice in the PSM and of a finite sampling size on the error in determining the statistical parameters of optical radiation in a random medium.

In a linear stationary random medium without absorption ($\varepsilon_{nl} = 0, \alpha = 0$), the transverse correlation function of the field $\Gamma_E(\mathbf{r}, \boldsymbol{\rho}, z)$ in the PSM has the same structure as in the case of a continuum [106]. The systematic error in the PSM, as estimated from Γ_E, is small provided the following condition is satisfied for the slab thickness in the model:

$$\Delta z \leqslant 2k_0h^2 . \tag{2.70}$$

This inequality specifies condition (2.14) written in the formulation of the PSM.

The quantitative estimate of the systematic error caused by the medium sampling over the coordinate z was obtained from analysis of the distribution of the average beam intensity. The relative error in the intensity calculation depends on the number J of screens in the PSM as follows:

$$\varepsilon_I \simeq \frac{1.5}{J} + \frac{0.5}{J^2} . \tag{2.71}$$

A similar estimate for the turbulent broadening Δ_{tJ}^2 of a beam scattered from a sequence of phase screens was obtained in [121]:

$$\Delta_{tJ}^2 = (1 + \varepsilon_I)\Delta_t^2 , \tag{2.72}$$

where Δ_t^2 is the turbulent broadening of a beam in a continuum.

A posteriori condition for the sampling interval Δz was formulated in [68]. According to this condition, the relative variance $\beta_I^2(\Delta z)$ of the intensity fluctuations in a slab should not exceed 0.1. In the case of weak fluctuations, when the variance $\beta_I^2(z_J) < 1$ over the entire propagation length, it is assumed that $\beta_I^2(\Delta z) \leqslant 0.1\beta_I^2(z_J)$.

2.3.2 Estimate of the sampling size. Practical estimates of the convergence of statistical parameters of optical radiation were made in [122] for the example of the test problem of propagation of a slit Gaussian beam through a medium with a Kármán spectrum of the dielectric constant fluctuations (2.53). In the case of weak fluctuations with the phase variance on a screen $\sigma_S^2 = 7 \times 10^{-3}$ (2.56), the mean intensity $\langle I(0)\rangle_N$ on the beam axis rapidly converges with increasing sampling size N (Fig. 5). As the variance σ_S^2 increases, the convergence of $\langle I(0)\rangle_N$ slows down.

The variance of intensity fluctuations $\sigma_I^2(r)$, as a high-order moment, is a statistical parameter which is more sensitive to the sampling size N. The establishment of the symmetric profile of $\sigma_I^2(r)$ in the isotropic field $\tilde{\varepsilon}(r)$ can be considered as a criterion for the convergence of the MCM. As was shown in [122], the sampling size of about 100 realizations provides a satisfactory accuracy of measuring the mean intensity $\langle I\rangle$ and variance σ_I^2 of a beam propagating along the atmospheric path in the case of a weak turbulence.

Notice that an increase in the number of screens J in the PSM results in additional averaging. When the condition $\sigma_S^2 J = \text{const}$ is satisfied, the increase in J results in the decrease in phase fluctuations on the screens and in the decrease of confidence intervals for estimating the statistic parameters of radiation over an ensemble containing a finite number N of realizations. Experience suggests that the PSM

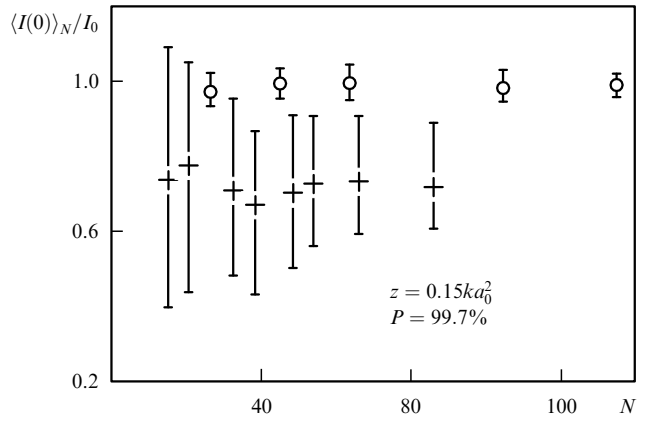

Figure 5. Convergence of the average intensity $\langle I(0)\rangle_N$ on the beam axis with increasing sampling size N in the MCM for the number of phase screens $J = 32$. The grid spacing $h = 5 \times 10^{-2} a_0$: (o) $\sigma_S^2 = 7 \times 10^{-3}$ ($C_\varepsilon^2 = 3 \times 10^{-15}$ cm$^{-2/3}$), (+) $\sigma_S^2 = 2 \times 10^{-1}$ ($C_\varepsilon^2 = 10^{-13}$ cm$^{-2/3}$).

with $J \geqslant 20$ provides the accuracy that is adequate for studying the problems of atmospheric optics [10, 68].

3. Partially coherent radiation in a regular medium

3.1 Self-modulation of a noise pulse

The self-modulation of a noise pulse in a medium with Kerr nonlinearity possesses a classical problem of nonlinear statistical optics. In the analytic study of this problem, the assumption of the statistically stationary light field and the nonaberrational approximation for a pulse with the mean envelope of a Gaussian shape are involved [1, 15]. The MCM allows one to abandon these assumptions.

3.1.1 Similarity parameters. In a regular medium with Kerr nonlinearity in the absence of absorption, Eqn (2.7) for the complex amplitude of a plane light wave takes the form

$$2ik_0 \frac{\partial \widetilde{E}(z,t)}{\partial z} = -k_0 \frac{\partial^2 k}{\partial \omega^2} \frac{\partial^2 E(z,t)}{\partial t^2} + k_0^2 \frac{\varepsilon_0 |\widetilde{E}^2|}{\varepsilon} \widetilde{E}(z,t) . \quad (3.1)$$

Propagation of the input pulse $\widetilde{E}_0(t)$ in the form of a narrowband Gaussian noise (2.44)–(2.47) is determined by two similarity parameters: the propagation length $z/\widetilde{L}_{\rm dp}$ expressed in units of the dispersion length $\widetilde{L}_{\rm dp}$ of the noise pulse and by the parameter $\widetilde{R}$ that characterizes the averaged nonlinear phase accumulation. According to [59, 124], the dispersion length $\widetilde{L}_{\rm dp}$ is equal to

$$\widetilde{L}_{\rm dp} = \frac{L_{\rm dp}}{2\sqrt{N}} , \quad N = \frac{1}{4} + \left(\frac{t_{\rm p}}{\tau_{\rm c0}}\right)^2 , \quad (3.2)$$

where $L_{\rm dp} = t_{\rm p}^2/|\partial^2 k/\partial \omega^2|$ is the dispersion length of the regular pulse of duration $t_{\rm p}$.

The nonlinearity parameter $\widetilde{R}$ of a statistical problem is determined from analysis of the approximate solution for the field coherence function $\Gamma(t, \tau, z)$ by assuming that the normal distribution of intensity fluctuations is conserved upon the self-action [124]:

$$\widetilde{R} = \frac{R}{N} , \quad (3.3)$$

where $R = L_{\rm dp} k_0 \varepsilon_2 A_0^2/\varepsilon$ is the nonlinearity parameter in the determinate problem [125]. One can see from (3.2) and (3.3) that as the correlation time $\tau_{\rm c0}$ decreases, so does the parameter $\widetilde{R}$ which determines the averaged nonlinear phase accumulation.

It follows from the solution to the equation for the function $\Gamma(t, \tau, z)$ obtained in the nonaberrational approximation [124] that for $\widetilde{R} < 1$, the average pulse duration $t_{\rm p}(z)$ and the correlation time $\tau_{\rm c}(z)$ increase monotonically with a distance because of dispersion and nonlinear self-modulation. For $\widetilde{R} > 1$, the values of $t_{\rm p}(z)$ and $\tau_{\rm c}(z)$ change periodically with the distance z. For $1 < \widetilde{R} < 2$, the pulse compression is small, and $t_{\rm p}(z)$ and $\tau_{\rm c}(z)$ remain greater than their initial values $t_{\rm p}$ and $\tau_{\rm c0}$. For $\widetilde{R} > 2$, the pulse is periodically compressed upon its propagation. The critical value of the parameter $\widetilde{R}_{\rm cr} = 2$ corresponds to the propagation regime in which the pulse compression caused by its self-modulation is on average compensated by the dispersive spreading.

The method of moments was used [21] to obtain the critical nonlinearity parameter $\widetilde{R}_{\rm cr}$ at which the mean-square duration of noise pulse (2.46) does not change upon its propagation:

$$\widetilde{R}_{\rm cr} = \frac{\sqrt{2}(1 + \sigma^2 + 4\sigma^2 t_{\rm p}^2/\tau_{\rm c0}^2)}{1 + 4\sigma^2 + 2\sigma^4} . \quad (3.4)$$

In this case, $\sigma^2 = 1$ for a Gaussian noise (2.44). The value of $\widetilde{R}_{\rm cr}$ estimated from (3.4) is 15–20% lower than the value obtained in the nonaberrational approximation in a broad range of ratios $\tau_{\rm c0}/t_{\rm p}$.

3.1.2 Field coherence. The degree of coherence $\gamma_N(t, \tau, z)$ is determined in the MCM by averaging over an ensemble of realizations $\{\widetilde{E}^{(i)}(t, z),\ i = 1, \ldots, N\}$ according to the equation

$$\gamma_N(t, \tau, z) = \frac{\langle \widetilde{E}(t - \tau/2, z)\, \widetilde{E}^*(t + \tau/2, z)\rangle_N}{\left(I_N(t - \tau/2, z)\, I_N(t + \tau/2, z)\right)^{1/2}} . \quad (3.5)$$

In a linear medium ($\widetilde{R} = 0$), the modulus $|\gamma_N(0, \tau, z)|$ of the degree of coherence in the pulse centre broadens monotonically with the distance z and retains its initial Gaussian shape (Fig. 6), which corresponds to analytic estimates [1]. The

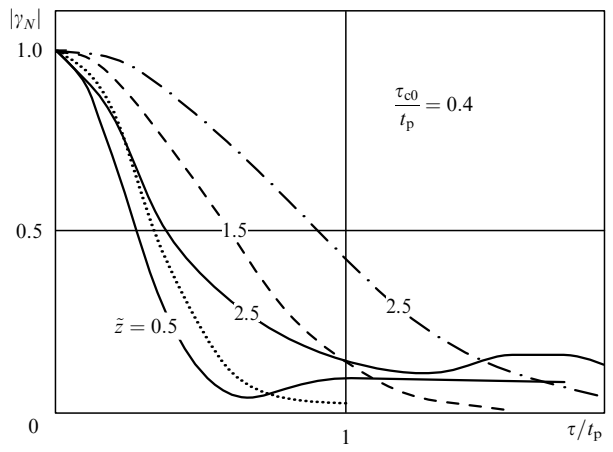

Figure 6. Modulus of the degree of coherence $|\gamma_N(0, \tau, z)|$ at the center of a noise pulse: (...) incident radiation, (- - - and – · –) linear case, (—) self-modulation in a supercritical regime with $\widetilde{R} = 3$ [124].

values of the coherence time τ_c calculated by the MCM at the pulse centre $t = 0$ and at its fronts $t = \pm t_p$ coincide. Therefore, the light field of the pulse remains quasi-stationary in a linear medium, the coefficient of coherence being constant: $\tau_c(z)/t_p(z) = \text{const}$.

Under conditions of nonlinear decompression ($\widetilde{R} < 0$), the function $|\gamma_N(0, \tau, z)|$ broadens stronger. In a supercritical regime ($\widetilde{R} > 2$), the profile of $|\gamma_N(\tau)|$ sharply narrows at short distances $z \sim 0.5\widetilde{L}_{dp}$ and again broadens during further propagation. The shape of the function $|\gamma_N(\tau)|$ is distorted and for $z \simeq 2\widetilde{L}_{dp}$ a slowly decaying 'tail' appears at $\tau \geqslant 0.3t_p$.

Despite the fact that the function $|\gamma_N(\tau)|$ substantially differs from a Gaussian one, we can estimate the coherence time τ_c at the e^{-1} level:

$$\left|\gamma_N\left(t, \tau_c(t, z), z\right)\right| = e^{-1}\left|\gamma_N(t, 0, z)\right| . \tag{3.6}$$

In a supercritical regime ($\widetilde{R} > 2$), the field coherence decreases sharply at short distances $z < 0.5\widetilde{L}_{dp}$ and then slowly increases (Fig. 7). The decrease in τ_c in the initial stage of propagation is caused by the decay instability of the noise field and a formation of subpulses. The subsequent increase in the coherence results from formation of solitons and simultaneous dispersive spreading of the noise nonsoliton component into a pedestal. As the nonlinearity parameter increases ($\widetilde{R} = 15$), the coherence time τ_c decreases more rapidly.

Notice that the nonlinear phase modulation is the most substantial at the pulse centre. This results in a violation of the statistical stability of the field, which is especially significant in a supercritical regime.

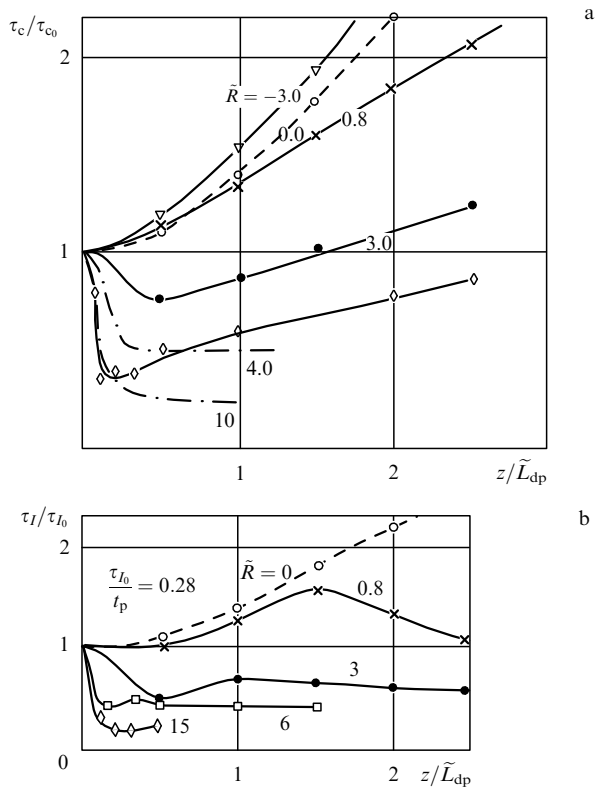

Figure 7. Change in the correlation scale of a partially coherent pulse upon self-modulation in a medium with cubic nonlinearity: solid and dashed lines — [124]; dot-and-dash lines — [128]; (a) the field coherence time $\tau_c(z)$, (b) the correlation time $\tau_I(z)$ of intensity fluctuations.

The nonmonotone change in τ_c with the distance z is also observed upon the self-modulation of picosecond noise pulses in an optical fiber, when the nonstationary response of a nonlinear medium [126] or the third-order dispersion [127] are substantial. In a subcritical regime ($\widetilde{R} < 2$), the field coherence increases monotonically with the distance z, more than usual strongly in the case of nonlinear decompression of the pulse, when $\widetilde{R} < 0$.

In [128], it has been found for the problem of self-focusing of a two-dimensional (slit) beam that the field correlation scale r_c decreases with the distance z for any $\widetilde{R} > 1$ (Fig. 7a). In this case, r_c decreases monotonically in a supercritical regime and tends to the stationary value, which the authors [128] explain by the small-scale self-focusing. However, upon fragmentation of the two-dimensional beam or formation of solitons, their parameters oscillate in the pulse with the distance z [125, 129]. It seems likely that the discrepancy between the results obtained in [128] and [124] are explained by errors in the numerical experiment [128] due to the frequency aliasing upon the nonlinear enrichment of the light spectrum in the absence of buffer zones.

Statistical studies of the pulse compression by means of a diffraction grating compressor showed [127] that the degree of compression of a partially coherent pulse decreases approximately by 30% as compared to that of a regular pulse.

3.1.3 On applicability of analytic methods. The analytic solution for the coherence function $\Gamma^a(t, \tau, z)$ may be obtained by using three independent approximations [1, 15]. The first approximation assumes that the Gaussian statistics is preserved upon the self-action of the light field, which allows one to obtain a closed equation in the coherence function $\Gamma^a(t, \tau, z)$. The second approximation consists in the parametric definition of the required function $\Gamma^a(t, \tau, z)$ as a self-modelling solution at which the field is assumed to be statistically stationary. Finally, the third approximation represents a parabolic approximation of the pulse shape in the vicinity of a point $t = 0$, which is necessary for determining the parameters of this solution. The latter assumption corresponds to the well-known near-axis approximation in the problem on the self-action of a light beam [125].

Analysis of the numerical solution to the closed equation for the coherence function $\Gamma(t, \tau, z)$ shows that the basic assumption of retention of the Gaussian statistics for the light field in a nonlinear medium is valid for a weak nonlinearity, when the parameter $\widetilde{R}$ does not exceed unity [124]:

$$|\widetilde{R}| < 1 . \tag{3.7}$$

In this case, the wave process of gaussisation of field fluctuations upon dispersion and diffraction dominates over nonlinear self-modulation of the phase. This condition is sufficient for the nonaberrational approximation to be applied, because nonlinear distortions of the mean intensity profile are small.

In [130], the equation in the coherence function of the axially-symmetric and purely-coherent light beam was numerically investigated in a cubic medium under condition (3.7). It was shown that the statistical isotropy of the light field was violated for $R = 10$ and the inhomogeneity parameter $N = 16$. At the beam axis, where the nonlinearity is substantial, the coherence radius decreases, whereas it increases at a periphery because of the diffractive divergence.

3.1.4 Distribution laws. The MCM analysis of the distribution function characterizing the light-field fluctuations was performed in [27, 124, 128, 131]. In a linear medium, the Gaussian statistics of the field is preserved. In a subcritical regime ($\widetilde{R} < 2$), the distribution of the quadrature components only slightly differs from the normal distribution.

In a supercritical regime ($\widetilde{R} \simeq 3$), the statistics of $\mathrm{Re}\,\widetilde{E}$ and $\mathrm{Im}\,\widetilde{E}$ changes qualitatively [124]. Analysis according to the goodness-of-fit test χ^2 [132] shows that the significance level α, for which the hypothesis of the normal distribution of the field quadrature components can be accepted, decreases with increasing z and the nonlinearity parameter $\widetilde{R}$. While for $\widetilde{R} = 0.8$, the significance level $\alpha = 0.3 - 0.5$ for $z = (1.0-1.5)\widetilde{L}_{\mathrm{dp}}$, then for $\widetilde{R} = 3$, the significance level $\alpha < 0.01$ for the same distance z.

When analyzing transformations of distribution functions for parameters of the light field, it is convenient to use the probability scale, in which these functions coincide with a bisectrix of the first coordinate angle. For example, the Rayleigh distribution scale makes this scale for the field modulus $|E|$ [1]:

$$\Phi_{(y)} = \int_0^y \eta \exp\left\{-\frac{\eta^2}{2}\right\} \mathrm{d}\eta\,, \quad \eta = \sqrt{\frac{\pi}{2}}\,\frac{|E|}{\langle |E| \rangle}\,. \tag{3.8}$$

In the case of nonlinear pulse decompression ($\widetilde{R} < 0$), the probability density increases at $y \sim 1-2$, i.e. for the field amplitude $|E|$ that is close to the mean value $\langle |E| \rangle$ (Fig. 8). This change is caused by smoothing of a random substructure of the noise pulse envelope [133]. For $\widetilde{R} > 0$, the probability of small values of the field amplitude $|E| < \langle |E| \rangle$ increases, this increase being small in a subcritical regime ($\widetilde{R} < 2$). For $\widetilde{R} > 2$, when the nonsoliton component forms a pedestal, the probability density for small amplitudes substantially increases and that for the values of $|E|$ close to $\langle |E| \rangle$ decreases at a time. It follows from the normalization of the distribution function $\Phi(|E|)$ that the change in $\Phi(|E|)$ at $\widetilde{R} > 2$ is accompanied also by an increase in the probability density for large amplitude outbursts with $|E| > \langle |E| \rangle$, which corresponds to the formation of solitons.

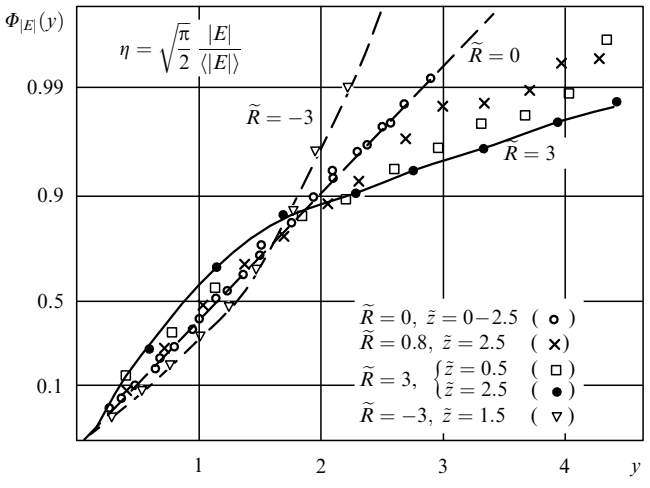

Figure 8. Transformation of the distribution function $\Phi_{|E|}(y)$ for the field modulus upon self-modulation of a partially coherent pulse in a medium with cubic nonlinearity [133]. The probability scale of the Rayleigh distribution is used along the ordinate axis.

Thus, during nonlinear processes of self-compression and spreading of the noise pulse ($|\widetilde{R}| > 1$), the distributions of light-field fluctuations substantially change. The initial field statistics in a nonlinear medium is not preserved, and the model of narrowband Gaussian noise proves to be invalid under conditions of the self-action.

3.1.5 Intensity statistics. The intensity $\langle I(t) \rangle_N$ obtained from the sampling of random realizations of the light field determines the mean shape of the noise-pulse envelope. In a nonlinear medium, the mean pulse duration $t_{\mathrm{p}}(z)$ increases with z independently of the nonlinearity sign [133]. For $\widetilde{R} < 0$, this is caused by self-demodulation, which, as dispersion, leads to the pulse spreading. For $\widetilde{R} > 2$, $t_{\mathrm{p}}(z)$ increases due to spreading of the nonsoliton component of the noise pulse and also due to a random drift of the pulse in 'running' time.

Delay in the nonlinear response results in some slowing down of the increase in a mean pulse duration $t_{\mathrm{p}}(z)$ [126]. In this case, the group delay of the pulse top appears, resulting in a substantially asymmetric pulse shape. As the coherence time $\tau_{\mathrm{c}0}$ becomes shorter, the relative contribution of the nonstationary self-action decreases because of the increased role of the dispersive spreading. The effect of the third-order dispersion is manifested in the asymmetric mean pulse shape and in the delay of the energy centre of the pulse [127]. As the duration of the input pulse decreases, the role of the higher-order dispersion increases and the relative value of the mean-square pulse duration increases faster with the distance z. In this case, a decrease in the coherence time $\tau_{\mathrm{c}0}$ accelerates spreading of the pulse in a nonlinear dispersing medium.

The correlation function of the intensity fluctuations is determined by the expression [123]

$$b_I(t,\tau) = \frac{\Big\langle \big(I(t+\tau/2) - \langle I(t+\tau/2)\rangle\big)\big(I(t-\tau/2) - \langle I(t-\tau/2)\rangle\big)\Big\rangle}{\Big[\big\langle (I(t+\tau/2) - \langle I(t+\tau/2)\rangle)^2\big\rangle \big\langle (I(t-\tau/2) - \langle I(t-\tau/2)\rangle)^2\big\rangle\Big]^{1/2}}\,. \tag{3.9}$$

The profile of the function $b_I(t^*,\tau)$ has a region of negative correlation, which is characteristic for randomly modulated waves and is located on the τ-axis near the coherence time τ_{c}. As the field coherence is improved, the region of negative correlation shifts toward higher values of τ for $\widetilde{R} \leqslant 0$. In a supercritical regime ($\widetilde{R} > 2$), the region of negative correlation first shifts toward lower values of τ because of the decay instability and the formation of subpulses, and then it shifts to greater τ in the process of soliton appearance and occurrence of a pedestal from the nonsoliton noise component. These regularities reflect the dependence of the correlation time $\tau_I(z)$ for the intensity fluctuations on the distance z. This time is usually measured at the e^{-1}-level of the function $b_I(0,\tau)$) (Fig. 7b) [133]. The asymptotic value of $\tau_I(z \to \infty)$ at $\widetilde{R} > 0$ is determined by the mean lifetime of a soliton and decreases with increasing nonlinearity.

The change in the probability density $w(I)$ of the intensity was obtained in [128] using the sampling of 1400 realizations for the problem on self-focusing of a two-dimensional beam. The formation of filaments in the two-dimensional beam at $\widetilde{R} = 10$ results in an increase in the probability density for large intensity deviations $I > \langle I \rangle$. A concurrent spreading of a 'pedestal' leads to an increase in the probability of small

fluctuations with $I < \langle I \rangle$. For $\widetilde{R} < 0$, the probability of moderate fluctuations $I \simeq \langle I \rangle$ grows due to nonlinear smoothing of random outbursts of the radiation intensity.

A comprehensive study of self-modulation of the noise pulse in a cubic medium with Kerr nonlinearity shows a close relation of changes in the coherence, the distribution functions for quadrature components, and the amplitude and intensity of the light field with the process of forming the waveguide regime during which solitons of the envelope are separated from the pulse and a 'pedestal' is formed.

In [134], the frequency spectrum of high-power subpicosecond laser pulses upon self-action in gases under conditions of Kerr and plasma nonlinearities was studied by the MCM. It was shown that in the case of Kerr nonlinearity the spectrum of a partially coherent pulse is on average smoothed and its shape is close to a Lorentzian one. As the intensity at the focus increases up to 10^{15} W/cm^2, when nonlinearity in a self-induced plasma dominates, an extended short-wavelength wing is formed in the pulse spectrum. A strong nonlinear dependence of the ionization rate on the intensity results in the appearance of two time scales of the coherence $\gamma(0, \tau)$.

3.2 Statistics of solitons

Problems of the formation and stability of solitons upon random perturbations are of great importance in the relay of information along optical fibres. The case of a weak nonlinear optical interaction of the noise field can be treated analytically. Under the assumption of the Gaussian statistics of optical radiation, the initial stage of the stationary pulse separation from a noise was investigated by the method of path integration [18, 135]. It was found with the method of inverse scattering problem that small fluctuations of the initial pulse amplitude affect only variations of the amplitude of the soliton formed, whereas phase fluctuations affect variations of its velocity [136, 137]. In the case of large fluctuations, the process of separation of a solitary pulse and statistical parameters of solitons formed are investigated by the MCM.

3.2.1 Formation of solitons. The process of forming the stationary pulse from a noise radiation is governed by Eqn (3.1). The input pulses with a Gaussian envelope are described by Eqns (2.47)–(2.50). The complex amplitude $\widetilde{E}_0(t)$ of a random field for input pulses of the soliton shape with a phase noise is written at $z = 0$ in the form [137, 138]

$$\widetilde{E}_0(t) = \sqrt{\frac{2A_0^2}{R}}\, N_c q_0 \operatorname{sech}\left(q_0 \frac{t}{t_p}\right) \exp\left[i\tilde{\varphi}(t)\right]. \tag{3.10}$$

For solitons with an additive Gaussian noise, Eqn (2.48) is rewritten in the form

$$\widetilde{E}_0(t) = \sqrt{\frac{2A_0^2}{R}}\, N_c q_0 \operatorname{sech}\left(q_0 \frac{t}{t_p}\right)\left(1 + \tilde{\alpha}(t)\right),$$

$$\tilde{\alpha}(t) = \tilde{c}(t) + i\tilde{d}(t), \tag{3.11}$$

where R is the nonlinearity parameter, q_0 is the form factor determining the amplitude and duration of a soliton, and N_s is the multiplicity of the soliton pulse.

The waveguide propagation regime exists under the condition $R = 2$, which yields the value of critical energy of the soliton formation [59]. The regular pulse ($\tilde{\varphi} = 0$, $\tilde{\alpha} = 0$) with the amplitude A_0, for which $R = 2$, forms a soliton at $N_s = 1$ and $q_0 = 1$. For the same value $R = 2$, the multiple increase in the field amplitude ($N_s = 2; 3$) results in the formation of the bound state of N_s solitons.

Numerical experiments with solitons [139] showed their stability relative to stationary deviations of the amplitude. If the amplitude perturbations $|\tilde{\alpha}| < 0.5$, then a soliton is formed from the pulse at $R = 2$ and $N_s = 1$ after several oscillations. For $\tilde{\alpha} < 0$, the establishment of the amplitude begins with its decrease. For $\tilde{\alpha} > 0$, the pulse amplitude first increases and then achieves the stationary value after several oscillations. The soliton amplitude established after the transient process is determined by the form factor, which is equal $q = 1 + 2\tilde{\alpha}$ for $|\tilde{\alpha}| < 0.5$. The multisoliton pulse ($N_s = 2; 3$) is also stable to small perturbations $|N_s\alpha| < 0.5$ [139].

Random intensity outbursts in noise pulses with the coherence time τ_{c0} comparable with the pulse duration t_p are 'picked up', in the case of a supercritical nonlinearity ($\widetilde{R} > 2$), by the nonlinear response of a medium. The wave decomposes, at the distance $z \simeq 0.1\widetilde{L}_{dp}$, into individual subpulses [124]. Then, at $z > 2\widetilde{L}_{dp}$, after several oscillations of their amplitude and duration, solitons are formed from the subpulses with energies exceeding the critical energy. The subpulses with energies lower than the critical energy spread and form a 'pedestal'. As a result, solitons are 'purified' of the noise. In [140], numerical studies were performed on the dynamics of a multisoliton pulse ($N_s = 16$) with an additive Gaussian noise (3.11) in a broad range of the coherence time ($\tau_{c0}/t_p = 0.03-0.48$) and noise variance ($\langle\tilde{\alpha}^2\rangle^{1/2} = 0.05-0.17$). It was found that at the initial path $z < L_{dp}$, either the initial pulse disintegrates into a sequence of individual pulses because of the amplitude-modulation instability or a solitary narrow pulse with the distorted shape is formed.

Analysis of the noise pulses propagation in a nonlinear medium at the distance z, which considerably exceeds the dispersion length L_{dp}, involves serious computational problems. This is explained by the fact that the region covered by the noise separated from a soliton extends with the distance z, and the dimensionality of numerical arrays describing the process excessively grows. Restriction of the region in which the pulse is considered is equivalent to the passage to the problem on a soliton against the noise background, the latter being formed upon repeated reflection of the noise waves from the region boundaries. The numerical experiment of this type reflects, in a some degree, the soliton dynamics in an optical fiber upon reflection of the stochastic waves from splitters and other optical elements.

The propagation of soliton pulses at $R = 2$ and $q_0 = 1$ with random δ-correlated amplitude and phase fluctuations (3.10) and (3.11) under conditions of the noise background was considered in [138, 141] for distances $z = (30-70)L_{dp}$. In the case of a weak phase noise with the variance $\sigma_\varphi^2 \leqslant 0.25$, a one-soliton pulse ($N_s = 1$) acquires a small random velocity, its amplitude and duration being changed insignificantly. The effect of the noise background is heightened with increasing variance. For $0.2 \leqslant \sigma_\varphi^2 \leqslant 1$, the pulse becomes randomly modulated and its maximum amplitude decreases, while its duration increases. The value of variance $\sigma_\varphi^2 = 1$ is critical for the existence of a one-soliton pulse.

As the phase-noise variance increases, a two-soliton pulse ($N_s = 2$) disintegrates into two individual solitons, which are moving apart, the bound two-soliton state being destroyed

(Fig. 9) [138]. When the noise variance exceeds $\sigma_\varphi^2 = 0.25$, the two-soliton pulse ($N_s = 2$) produces a single soliton with weak fluctuations of the shape.

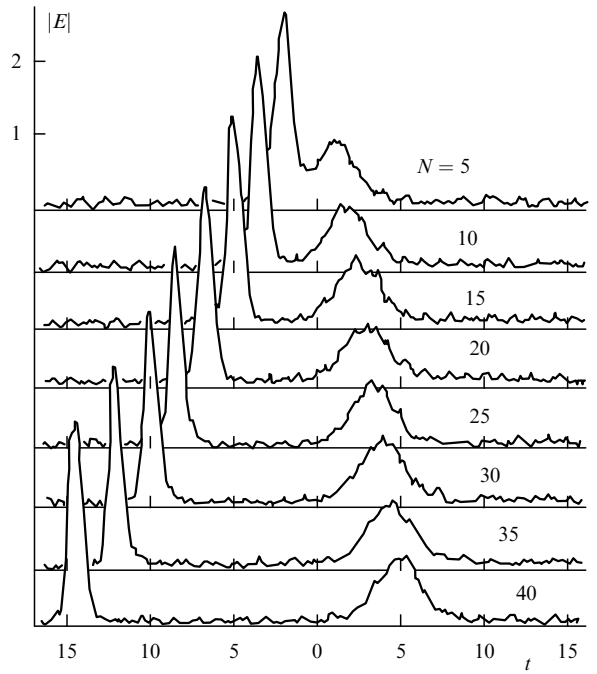

Figure 9. Decay of the bound two-soliton state. The evolution of a pulse with phase noise (3.11) for $N_s = 2$, $R = 2$, $q_0 = 1$, $\sigma_\varphi^2 = 6.87 \times 10^{-2}$. The time and the distance z are expressed in units of t_p and L_{dp}, respectively [138].

Soliton pulses are more stable to a random amplitude modulation ($\mathrm{Re}\,\tilde{\alpha} \neq 0$, $\mathrm{Im}\,\tilde{\alpha} = 0$). The critical parameter of the one-soliton pulse existence is the value of variance of amplitude fluctuations $\sigma_\alpha^2 = 1.7$. For two individual solitons, $\sigma_\alpha^2 = 0.25$.

The frequency spectrum $\widetilde{E}(\omega)$ of one-soliton stochastic pulses exhibits regions of a random modulation, which appear because of the interaction of propagating pulses with the noise waves formed upon soliton 'purification' [142].

Notice that in numerical studies [138, 141, 142], the specific results were obtained, which substantially depend on the region size $\mathcal{L}_t$ determining the noise level and, hence, the effect of stochastic waves on the formation and 'purification' of solitons. In addition, the use of a δ-correlated noise can result in significant errors because the numerical scheme does not reproduce the high-frequency enrichment of the spectrum whose upper edge coincides with the Nyquist frequency of a network.

3.2.2 Statistics of soliton parameters. The method of inverse scattering problem [143] is more efficient for the statistical estimate of parameters of solitons formed from a noise pulse. In [144], the algorithm was developed for calculating the solition spectrum for a single realization of the input pulse with perturbations of the general type. This permitted the use of the MCM for determining the mean values and deviations of the form factor q and the soliton velocity [137, 145].

For the N_s-soliton pulse with additive Gaussian noise (3.11), an increase in the noise amplitude σ_α results in the increase of form factors q, which is explained by an increase in the mean pulse energy proportionally to $1 + \sigma_\alpha^2$. Figure 10 shows σ_α-dependent mean values and standard deviations of form factors q obtained from the sampling containing 256 realizations for the three-soliton pulse with the noise coherence time $\tau_{c0} = 0.5 t_p$ [145]. The form factor q increases most significantly for the lowest component of the soliton spectrum, which is explained by a comparatively long noise correlation time. For $\sigma_\alpha \simeq 0.6$, the values of q for two lowest soliton components coincide. This corresponds to the unstable degenerate state in which two solitons of equal amplitudes greatly differ in their velocities.

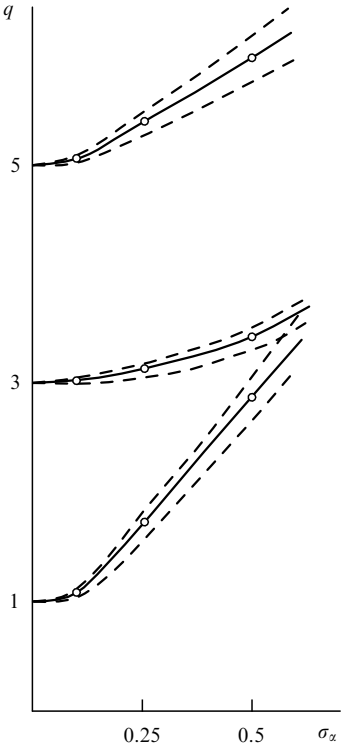

Figure 10. Dependences of average values and standard deviations of form factors q for different components of a three-soliton pulse on the noise amplitude σ_α [145].

For the low noise level $\sigma_\alpha \leqslant 0.25-0.50$, standard deviations of the form factor and soliton velocity depend linearly on the noise amplitude σ_α, which coincides with analytic perturbation calculations. As experiments with one-soliton pulses show [137], this linear dependence is violated with increasing σ_α, and fluctuations of soliton parameters grow more significantly. In the case of one-soliton pulses with a high noise amplitude ($\sigma_\alpha \simeq 0.5-1.0$), the probability of the appearance of solitons with lower form factors increases.

3.3 Nonstationary self-action of beams

Upon propagation of the pulse radiation through absorbing media, the light field induces perturbations of the dielectric constant ε_{nl}, which are changing in time because of the heat and mass transfer. The nonlinear response of the absorbing medium is not instant and is not localized in space. This fact is reflected in the appearance of spatial and time dispersion of the nonlinear contribution of the dielectric constant ε_{nl}.

In the isobaric approximation ($t_p > a/c_s$, where c_s is the sound velocity), the establishment of temperature is char-

acterized by time scales related to the convection ($\tau_{va} = a/v$ and $\tau_{vr} = r_c/v$) and thermal conductivity ($\tau_{\chi a} = a^2/4\chi$ and $\tau_{\chi r} = r_c^2/4\chi$) within the beam dimensions a and over spatial inhomogeneities of size r_c. For short pulses τ_c, $t_p < \tau_\chi$ in an immobile medium ($v = 0$), the model of localized nonlinearity is valid, in which heat transfer caused by convection and thermal conductivity is negligible during the course of the pulse. Constitutive equation (2.10) takes the form [146, 147]

$$\varepsilon_{nl} = \frac{\partial \varepsilon}{\partial T} T, \quad \rho c_p \frac{\partial T}{\partial t} = \alpha_{abs} I. \tag{3.12}$$

The approximation of localized nonlinearity is used in analysis of the self-action of femto- and subpicosecond laser pulses with power densities of $10^{13} - 10^{15}$ W/cm^2 in gases under conditions of ionization [148, 149]. This approximation is valid when the effect of electron diffusion, pondermotive forces, and ion recombination on the electron concentration distribution $N_e(\mathbf{r}, z, t)$ is small during the course of the pulse. A set of constitutive equations is written in the form

$$\varepsilon_{nl} = -\frac{\omega_p^2}{\omega^2}, \quad \omega_p^2 = \frac{e^2 N_e}{\varepsilon_0 m},$$
$$N_e = \sum_k k N_k, \quad \frac{dN_k}{dt} = -R_k(I) N_k + R_{k-1}(I) N_{k-1}, \tag{3.13}$$

where N_k is the concentration of ions of the kth multiplicity, and $R_k(I)$ is the ionization rate which depends on the intensity I.

In moving media, the thermal conductivity dominates for $\tau_\chi < \tau_v$, and convection for $\tau_\chi > \tau_v$ [150].

When power of a beam propagating in the vertical direction in an immobile medium is sufficiently high, the self-induced convection develops and a perturbation is mainly caused by the longitudinal heat transfer [151].

Upon nonstationary self-action of the beams under conditions of thermal and plasma nonlinearities, the dispersive spreading of a pulse is negligible. In this case, the subject for study is the dynamics of spatial fluctuations of radiation and time variation of the spatial statistics of the light field.

3.3.1 Development of aberrations. Space-time instability. The dynamics of light-field fluctuations is qualitatively reproduced by the time variation of a random irregular profile of partially coherent beam (2.52) [122, 146, 147]. At the leading edge of a pulse ($t \simeq 0.1 t_p$), a nonlinear suppression of random intensity maxima occurs because of their local defocusing at the induced inhomogeneities of a medium (Fig. 11). Upon local thermal self-action, a strong correlation exists between inhomogeneities induced in a medium and perturbations of the light field. According to notions [152], a 'specklon' is formed at the leading edge of the pulse, and radiation inhomogeneities are suppressed 'resonantly in space' by corresponding speckle inhomogeneities of the medium. This results in the efficient defocusing of local intensity maxima, their width being increased and amplitude being decreased. Such a weakening of the light field inhomogeneities occurs at small perturbations [153].

The optical strength of random thermal lenses in a medium increases with time ($t \simeq 0.3 t_p$) and aberrations appear caused by the beams caustics. For this reason, along with continuing spreading of the intensity outbursts, their fragmentation starts.

This results from the space–time instability of radiation in a defocusing medium with dispersion of the nonlinearity.

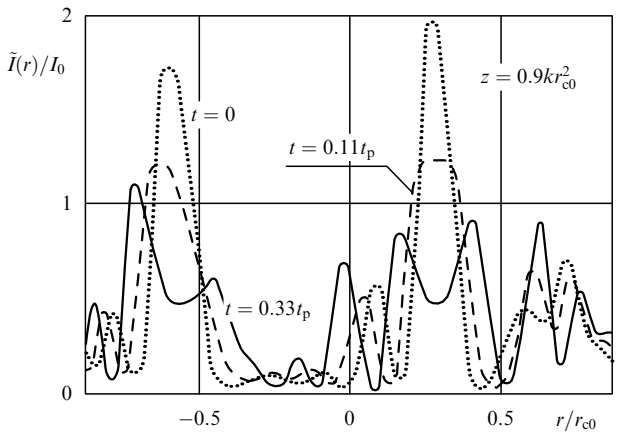

Figure 11. Development of aberrations in the intensity profile $I(r)$ upon nonstationary thermal self-action of a beam scattered by a phase screen. The characteristic size of speckle inhomogeneities $r_I = 0.5 r_{c0}$ and the critical time $t_{cr} = 0.36 t_p$ [147].

The time t_{cr}, at which small-scale fluctuations of the field appear, can be estimated from the condition of equality between the energy that passed through the cross section of the speckle inhomogeneity of the field and the critical energy of thermal self-action.

Upon the nonstationary thermal self-action of a beam, the longitudinal transfer of the nonlinearity accumulated in time occurs in a medium moving in the direction of the beam propagation. This can result in the formation of another positive feedback applied to perturbations of the temperature and light field [154].

Under conditions of ionization in gaseous media, a change in the refractive index is determined by its dependence on the intensity, which is stronger than those for Kerr or thermal nonlinearities. For this reason, large space–time gradients of the refractive index appear in the field of a high-power ultrashort laser pulse, and the light-field instability develops more rapidly. An initial Gaussian beam takes a circular structure because of a strong aberration defocusing at the boundary of the near-axis region, where the electron concentration N_e in a self-induced plasma is maximum. The nonlinearity is accumulated with time and the beam decomposes at the trailing edge of the pulse into a complicated system of rings [155].

Dynamic distortions in a spatial structure of the ultrashort laser beam are indissolubly related to the change in the frequency spectrum of the pulse [156]. In the region of rings on the beam profile, where a gradient of the refractive index is maximum, the spectrum is considerably shifted to the blue.

In resonance media, the pulse decomposes into solitary circular waves, which diverge from the beam axis, resulting in the induction of conical radiation emission [157]. The dynamics of spatial, time, and spectral distributions over the light field of the high-power laser pulse in a resonance medium was considered at length in [158, 159]. It was shown that the frequency-angular spectrum instability develops in the pulse for any sign of detuning the fundamental frequency off the resonance.

The space–time light-field instability in media with dispersion of the nonlinearity can be defined as a 'dynamic instability', which is substantially determined by phase relations between perturbations of the light field and the refractive index of the medium. The beam filamentation in the

case of small-scale self-focusing in the Kerr medium with an instant nonlinear response [3] represents a 'static instability' or 'divergence' of the light field.

Analysis performed by the perturbation method [12] showed that the dynamic instability in the Kerr medium develops upon the simultaneous manifestation of diffraction and dispersion effects, which accomplish the space – time relationship in the nonlinear distributed 'radiation – medium' system.

3.3.2 Spatial coherence. The spatial coherence function $\gamma(-r/2, r/2, t)$ of the field is determined by the MCM from the expression similar to (3.5).

Upon defocusing of the local intensity maxima at the pulse leading edge ($t \simeq 0.1t_p$), the function $|\gamma(-r/2, r/2, t)|$ for a beam scattered from phase screen (2.52) broadens, which suggests that the spatial field coherence improves [160]. When small-scale fluctuations appear at $t \simeq t_{cr}$, the coherence deteriorates at small distances $r < r_{c0}$, where r_{c0} is the initial coherence radius. Simultaneously, the nonlinear divergence, similar to the diffractive one, increases the field correlation at large distances $r_c \simeq 2r_{c0}$. Then, the function $|\gamma(-r/2, r/2, t)|$ loses its unimodality. As the spatial instability of the light field is developing, the decorrelation is spreading over the entire cross section of the beam, and for $t > t_{cr}$, the radiation coherence is substantially impaired.

The correlation radius $r_c(t)$, which is determined from some level of the function $|\gamma(-r/2, r/2, t)|$, partially reflects a complicated transformation of the field coherence. This radius changes nonmonotonically with time (Fig. 12). An initial increase in $r_c(t)$ corresponds to the defocusing of local maxima and its subsequent decrease corresponds to the enrichment of the spatial spectrum of the field by higher-order harmonics under conditions of the space – time instability. The nonmonotone change of the correlation radius of the field in time obtained by the MCM was confirmed by laboratory studies of the spatial coherence upon thermal self-action of the beam scattered from the phase screen. Simultaneous numerical and laboratory experiments [160] showed that the temporal change in the spatial coherence substantially depends on the initial statistics of radiation. As the variance of amplitude fluctuations of the incident radiation increases, a relative upgrading in the coherence occurring at the leading edge of the pulse is diminished. In the case of well-developed speckles of the incident radiation, the coherence radius $r_c(t)$ of the output beam monotonically decreases with time upon the nonstationary thermal self-action.

3.3.3 Intensity statistics. Flattening of field fluctuations due to the local defocusing at the pulse leading edge and the subsequent development of aberrations result in the nonmonotone change of the intensity variance σ_I^2 in time (Fig. 12).

The coefficient $b_I(r)$ of spatial correlation of the intensity fluctuations is determined from statistical tests in line with the expression similar to (3.9). At the pulse leading edge ($t \simeq 0.1t_p$), the coefficient $b_I(r)$ broadens and the region of negative correlations shifts to greater values of the argument r [147]. As aberrations appear at $t \simeq t_{cr}$, the region of the positive correlations narrows. Simultaneously, an additional region of a strong correlation at distances $r \simeq 2r_{I_0}$ appears because of the continuing global broadening of initial intensity outbursts. The function $b_I(r)$ becomes an essentially two-scale function.

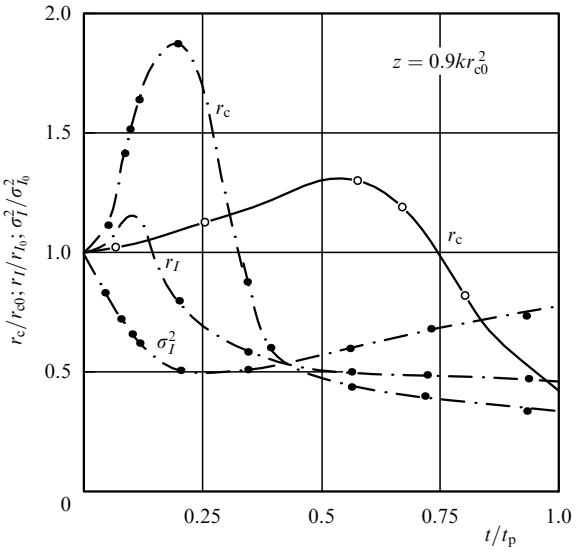

Figure 12. Time variations of statistical parameters (the coherence radius r_c of the field, correlation radius r_I, and intensity variance σ_I^2) for a partially coherent light beam upon nonstationary thermal self-action obtained (•) by the MCM and (o) in laboratory experiments [160].

The correlation radius $r_I(t)$ of the intensity fluctuations determined from a half-maximum level of the $b_I(r)$ profile increases at the pulse leading edge and then decreases (Fig. 12).

3.3.4 Spatial spectrum. The development of small-scale aberrations on the beam profile is manifested in the high-frequency enrichment of the spatial spectrum of the light field. At the pulse leading edge, the modulus $\langle|\Phi_E(\varkappa)|\rangle_N$ of the spectrum is unimodal, with the characteristic width $\varkappa_0$ (Fig.13) [147]. At the pulse trailing edge, the shape of the modulus is distorted and amplitudes of the Fourier harmonics substantially increase at frequencies by a factor of 2 – 3 higher than $\varkappa_0$. This reflects transfer of the field energy to the

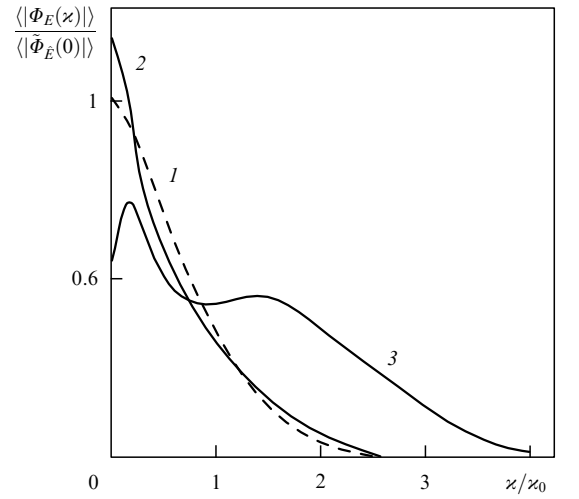

Figure 13. Transformation of the spatial spectrum of the field modulus upon nonstationary thermal self-action of a beam scattered by a phase screen for $t_{cr} = 0.36t_p$; $\varkappa_0$ is the upper bound of the spectrum in a linear medium; $t/t_p = 0$ (*1*); 0.11 (*2*); 1.0 (*3*) [147].

high-frequency components of the spatial spectrum under conditions of the space–time instability.

3.3.5 Multimode beam. Investigation on the spatial statistics of a beam from a pulsed multimode laser propagating under conditions of the nonstationary thermal self-action is based on the imitative model of radiation (2.67), (2.68). One can see from the isophotes for individual realizations that the spreading of speckles at the pulse leading edge and their subsequent fragmentation occur simultaneously with the global broadening of the beam (Fig. 4c, d) [161]. The region of the spatial localization of radiation, which is determined by the efficient radius $\langle a_{\text{eff}} \rangle_N$ of the beam, extends both due to diffraction (Fig. 4b) and thermal defocusing of the beam as a whole.

The spatial coherence of a multimode beam with well-developed speckles is diminished monotonically with time, in contrast to that of a beam scattered from a phase screen.

In a linear medium, a multimode beam with well-developed speckles can be compared with a regular Gaussian beam of the same divergence. However, an attempt to replace the statistical study of the self-action of a partially coherent beam by an equivalent determinate problem results in the error in estimates of the beam parameters. This is explained by the fact that the nonlinear defocusing of the partially coherent beam develops in a greater degree than that of the regular beam with averaged parameters because of the correlation between inhomogeneities induced in the medium and speckles of the light field.

3.4 Stimulated Raman scattering

Stimulated Raman scattering (SRS) relates to a nonlinear optical process which permits the conversion of laser radiation. Of great interest is the SRS conversion of laser radiation intended for narrowing its frequency spectrum and reducing the angular divergence of the laser beam. Physical aspects of the mechanism of the wavefront correction during the forward SRS conversion have been discussed in a review [162].

Computer experiments play a significant role in studies on the SRS conversion, in particular, those with random fields in studies of the SRS amplification in the incoherent pumping field.

In the approximation of coupled waves [57], the complex amplitudes of the pumping wave, $E_{\text{p}}(\mathbf{r}, z, t)$, and of the forward Stokes wave, $E_{\text{s}}(\mathbf{r}, z, t)$, are described by the system of equations

$$\begin{aligned}
&\frac{\partial E_{\text{p}}}{\partial z} + \frac{1}{v_{\text{p}}} \frac{\partial E_{\text{p}}}{\partial t} + \frac{\text{i}}{2k_{\text{p}}} \Delta_{\perp} E_{\text{p}} = \gamma_{\text{p}} E_{\text{s}} Q \,, \\
&\frac{\partial E_{\text{s}}}{\partial z} + \frac{1}{v_{\text{s}}} \frac{\partial E_{\text{s}}}{\partial t} + \frac{\text{i}}{2k_{\text{s}}} \Delta_{\perp} E_{\text{s}} = \gamma_{\text{s}} E_{\text{p}} Q^{*} + \tilde{\mu}_{\text{s}} \,, \\
&\frac{\partial Q}{\partial t} + \frac{Q}{T_2} = \gamma_{\text{q}} E_{\text{p}} E_{\text{s}} \,,
\end{aligned} \tag{3.14}$$

where $Q(\mathbf{r}, z, t)$ is the complex amplitude of the wave of molecular vibrational modes, $\gamma_{\text{p, s, q}}$ are the coefficients of the nonlinear interaction of radiation with the Raman-active medium, $\tilde{\mu}(\mathbf{r}, z, t)$ is the amplitude of noise, $v_{\text{p, s}}$ are the group velocities for pumping and Stokes waves, and $T_2 = 2\pi/\Delta\omega_0$, where $\Delta\omega_0$ is the Raman linewidth. System of equations (3.14) does not take into account the higher Stokes components and backscattering.

Analysis of the wavefront correction is usually performed in the stationary approximation ($t_{\text{p}} > T_2$), which assumes that $\partial Q/\partial t = 0$, $v_{\text{p}} = v_{\text{s}}$, and complex amplitudes of the fields only depend on spatial coordinates r and z. Correction of the frequency spectrum upon the SRS conversion is considered in the plane wave approximation, when $E_{\text{p, s}}$ depend on time and the longitudinal coordinate z.

3.4.1 Wavefront correction. The main idea of the wavefront correction consists in a space averaging of the Stokes radiation in the process of amplification in the incoherent pumping field. Such an averaging is achieved due to locality of the SRS effect, which is reflected in the absence of space derivatives in the equation for Q in (3.14). In other words, in the Raman-active medium the wave of molecular vibrational modes is formed with the width of the spatial spectrum overlapping the spectrum of incoherent pumping. For this reason, the pumping energy is efficiently transferred into the energy of a highly coherent Stokes beam.

In practice, the space averaging of the pumping intensity is performed by means of the prism or mirror integrator, which directs different paths of the pumping beam into the interaction region. In this case, the maximum efficiency of the SRS conversion up to 60% and above is achieved with the help of an aberrator, which first deteriorates the spatial coherence of the pumping.

A series of numerical experiments on the SRS amplification in a random field of the crossing incoherent pumping beams was performed in [91, 163] for a two-dimensional model. The SRS in compressed hydrogen upon pumping by a XeCl laser at $\lambda = 0.308\,\mu\text{m}$ was studied. Figure 14 displays the realization for a scheme with four crossing pumping beams whose divergence after an aberrator was higher than the diffractive divergence by a factor of 120. Each of the beams was modelled with a super-Gaussian profile of width 1.5 cm. Despite a randomly inhomogeneous distribution of the pumping intensity over the cross sectional area of the interaction region, the Stokes beam retained its near-Gaussian profile after amplification. The results of numerical simulation are in good agreement with experimental data.

3.4.2 Frequency-spectrum correction. The extension of the concept of averaging to the temporal dependence for obtaining the narrowband Stokes radiation in the broadband pumping field involves fundamental difficulties. The point is that the response of the Raman-active medium is not instant in contrast to its spatial localization. The phase of molecular vibrational modes depends on previous time instants, which is reflected by the term $\partial Q/\partial t$ in (3.14). The frequency spectrum of these modes, even in media with a broad Raman line $\Delta\omega_0$, is substantially narrower than the spectrum of the broadband pumping $\Delta\omega_{\text{p}}$. In this case, the coherence time of pumping τ_{cp} is considerably shorter than the relaxation time T_2, and its random phase fluctuations completely transfer to the Stokes radiation, whereas upon narrowband pumping, when $\tau_{\text{cp}} \gtrsim T_2$, the phase of the Stokes pulse only partially repeats random phase fluctuations of pumping. This is confirmed by the results of numerical experiments on the nonstationary forward SRS amplification of a start Stokes pulse in a random field of the nonmonochromatic pumping [92, 164].

Some narrowing of the output Stokes band as compared to the pumping band is also achieved upon SRS pumping in media with a significant dispersion of group velocities [162].

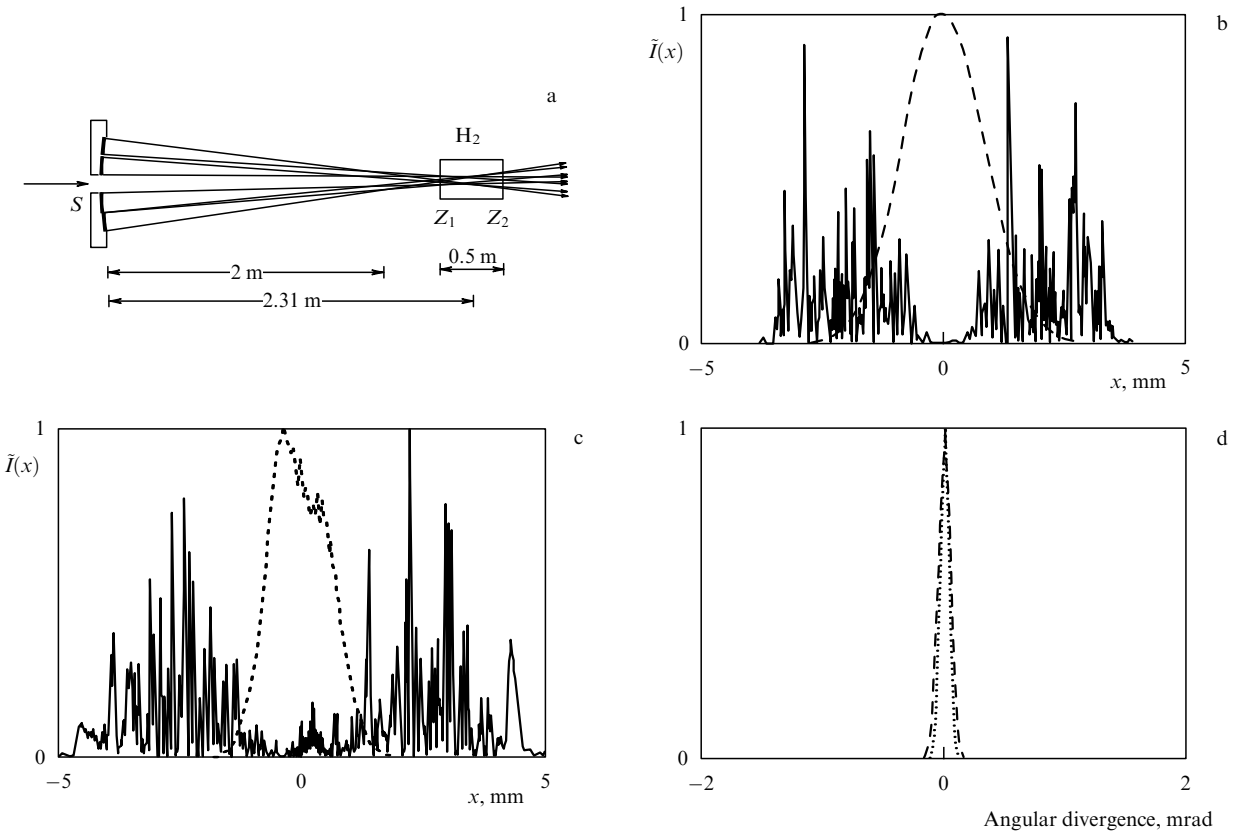

Figure 14. The intensity distribution $\tilde{I}(x)$ in a separate realization of the pump and Stokes beams for a SRS amplifier with four crossing partially coherent pump beams: (a) layout of the SRS amplification; (b) the pump (solid curve) and Stokes beams (dashed curve) in the entrance plane z_1; (c) the pump and Stokes beams in the exit plane z_2; (d) the Stokes beam in the far field: the input beam (dotted curve) and the amplified beam (dashed curve) [163].

In this case, the space – time averaging occurs during the shift of the Stokes pulse relative to the pumping pulse. However, the dispersion of group velocities is small and the coherence of the Stokes radiation improves only slightly. According to the results of statistical tests [92], the coherence time τ_{cs} of the output Stokes pulse is approximately one and a half times longer than the coherence time τ_{cp} of pumping, when the relative mismatch of group velocities v_p and v_s is equal to 0.02.

In the case of backward stimulated Raman scattering (BSRS), an opposing Stokes pulse moves within an inhomogeneous broadband pumping pulse, and efficient space – time averaging of fluctuations of the Stokes radiation induced upon amplification occurs. The mathematical problem on the nonstationary BSRS is described by system (3.14) with reversed sign on $\partial E_s/\partial z$.

Figure 15 shows an example of the random realization of the numerical experiment on amplification of a start Stokes pulse in the case of BSRS in the field of noise pumping [165]. During amplification of the Stokes radiation, the pumping pulse is depleted at its trailing edge. The output Stokes pulse retains its unimodal shape, its phase being monotonically changed despite the considerable phase fluctuations of pumping. According to the results of statistical analysis, the averaged shape of the amplified Stokes pulse is close to a Gaussian one. The variance of intensity is maximum at the leading edge of the pulse because of a random appearance of the intensity outbursts in the noise pumping. The coherence function changes negligibly in a time of the Stokes pulse, and the amplified BSRS radiation is in fact totally coherent. The degree of coherence of the output Stokes pulse is somewhat deteriorated under the conditions of a strong depletion of pumping. The average conversion efficiency grows with increasing coherence time τ_{cp} of pumping.

4. Light beams in the turbulent atmosphere

4.1 Classification of problems

The propagation of intense optical radiation in the atmosphere is accompanied by a simultaneous manifestation of nonlinear effects and fluctuations of the atmospheric parameters. The nonlinear refraction and large-scale turbulence cause random walk and defocusing of a beam. The thermal self-action of radiation in the field of small-scale fluctuations of the medium results in the broadening of the beam and transformation of its spatial statistics.

Studies on the propagation of light beams along atmospheric paths cover many problems which involve analysis both of the energy parameters determining the distribution of the light field power in space and time and of information parameters related to the radiation coherence and the level of fluctuations. The unified approach to these problems is based on the MCM, in which the propagation of the intense laser radiation along the atmospheric path is simulated with a computer.

4.1.1 Nonlinear effects. Nonlinear distortions, which appear upon propagation of intense light beams in the atmosphere, result from the interaction of radiation both with atmospheric gases and solid and liquid fractions of aerosol particles [5]. A

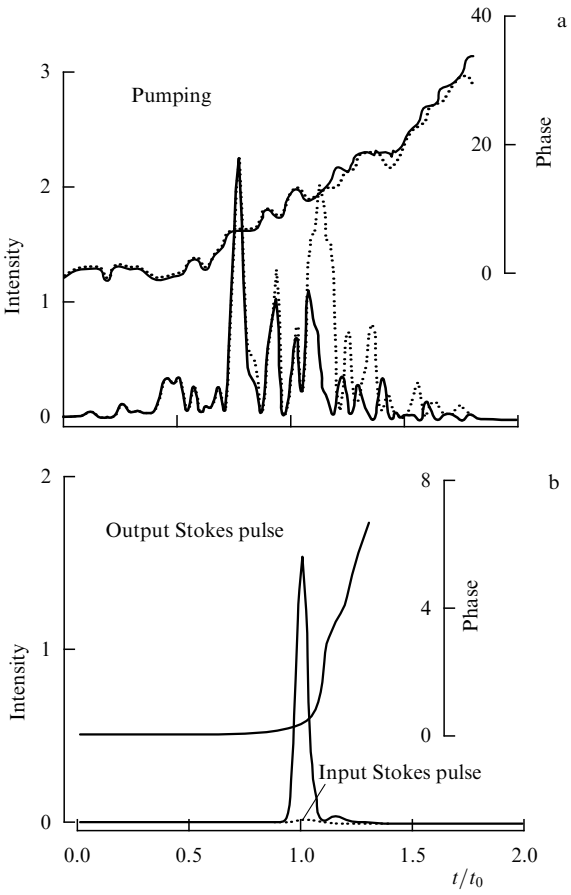

Figure 15. Intensities and phases of the pump and Stokes pulses in a random realization of amplification of the start pulse in the noise pumping upon backward SRS with the increment $G = 8$. The pump pulse duration is $t_p = 200$ ps, the coherence time of pumping $\tau_{cp} = 5$ ps, the input Stokes pulse duration and intensity are $t_s = 0.1t_p$ and $I_s = 0.01I_p$, the relaxation time $T_2 = 10$ ps, and the scale $t_0 = 230$ ps. The intensity is given in relative units and the phase, in radians [165].

phenomenon of the electrostriction, a change in the molecular polarizability [166], kinetic effects in the resonance interaction [167–169], perturbations of density and temperature [170–172] upon absorption of radiation cause the nonlinear refraction of the beams. The effects of nonlinear absorption in gases and aerosol [5] and blocking of the light field upon optical breakdown in air [173] give rise to the nonlinear attenuation of radiation. The effects of stimulated thermal scattering (STS), stimulated Brillouin scattering (SBS) [174, 175], and scattering by thermal aureoles near absorbing particles [173] increase the angular divergence of radiation. Nonlinear effects are related to different physical processes; they substantially depend on the radiation regime and meteorological conditions along the path [5]. Analysis [58] showed that in most practically interesting radiation regimes the nonlinear refraction upon thermal self-action exhibits the lowest energy threshold.

Time scales τ_{nl} characteristic of the nonlinear refraction usually satisfy the system of inequalities

$$\tau_s < \tau_\varepsilon < \tau_{\chi_\varepsilon} < \tau_{\chi_a} < T_v\,, \tag{4.1}$$

where τ_s is the time of establishment of pressure, τ_{χ_a} and τ_{χ_ε} are the times of the thermal conductivity on scales of the light beam and inhomogeneity of a medium, and T_v is the period of the wind-velocity pulsations. The convective time τ_v changes within a broad range.

Relations between the times of radiation interaction with a medium, t_p or τ_v, on the one hand, and time scales τ_{nl}, on the other, determine main nonlinear effects observed upon propagation of the light beam in the atmosphere. Thus, for pulses of duration $t_p \simeq 0.01$ s, the inequalities $\tau_s < t_p < \tau_v < T_v$ are valid, which permits the use of the isobaric model of the nonstationary local defocusing in an immobile random medium. In the long-pulse regime, when $\tau_v < t_p < T_v$, the wind refraction dominates, which develops in a flow of a random medium. In this case, the flow velocity can be considered constant and inhomogeneities of the refractive index can be treated as 'frozen'. In the case of quasi-continuous radiation with $t_p > T_v$, random walk and defocusing of the beam under conditions of the wind-velocity pulsations are the dominant factors.

In the above regimes, the amplitude of the field $E(\mathbf{r}, z, t)$ in the aerosol-free turbulent atmosphere is described by the system of equations

$$2ik_0\frac{\partial\widetilde{E}}{\partial z} = \Delta_\perp\widetilde{E} + \frac{k_0^2}{\varepsilon}\frac{\partial\varepsilon}{\partial T}\widetilde{T}\widetilde{E} + k_0^2\frac{\tilde{\varepsilon}}{\varepsilon}\widetilde{E} - ik_0\alpha\widetilde{E}\,,$$
$$\frac{\partial\widetilde{T}}{\partial t} + \mathbf{v}\nabla_\perp\widetilde{T} = \alpha(\rho c_p)^{-1}\widetilde{I}\,, \tag{4.2}$$

combined with the condition of the 'frozen' turbulence [123]

$$\tilde{\varepsilon}(\mathbf{r}, z, t+\tau) = \tilde{\varepsilon}(\mathbf{r} - \mathbf{v}\tau, z, t)\,. \tag{4.3}$$

4.1.2 Similarity parameters. In the numerical experiment, it is convenient to use the variance σ_J^2 of the phase perturbations, determined on twice the diffraction length $2L_{df}$, as the similarity criterion characterizing fluctuations of the dielectric constant of the medium [10]. In the model of phase screens whose variance is determined from (2.56), the criterion σ_J^2 is equal to

$$\sigma_J^2 = 1.8\times10^{-2}C_\varepsilon^2k_0^3L_0^{5/3}a_0^2\,. \tag{4.4}$$

The nonlinear refraction of a beam caused by the thermal self-action is characterized by the nonlinearity parameter R:

$$R = \frac{k_0^2a_0^2}{\rho c_p n_0}\left|\frac{\partial\varepsilon}{\partial T}\right|w_\alpha\,. \tag{4.5}$$

The characteristic density w_α of the absorbed energy is equal to

$$w_\alpha = \int_0^t \alpha_{abs}\,I_0(t)\,dt \tag{4.6}$$

for the pulse duration $t_p < \tau_v$, and

$$w_\alpha = \frac{\alpha_{abs}\,I_0a_0}{v} \tag{4.7}$$

for $t_p > \tau_v$ and quasi-continuous radiation.

A direct comparison of the parameters of turbulence σ_J^2 and nonlinearity R allows one to estimate qualitatively which factor dominates in distortions of light beam in the atmospheric path. An example of a realization obtained for $R < \sigma_J^2$ is presented in Fig. 16, where the intensity distribution over the cross section of the beam propagating in the atmosphere is

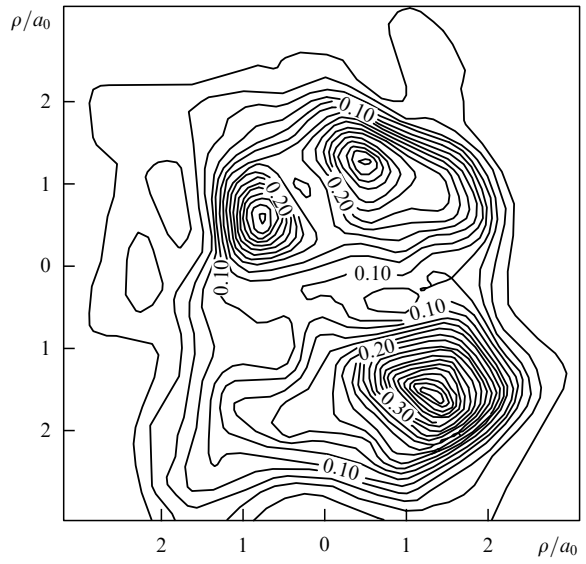

Figure 16. The intensity distribution at the cross section of a beam propagated to the distance $z = 0.5ka_0^2$ in the turbulent atmosphere with spectrum (2.53). The beam radius is $a_0 = 10$ cm, the wavelength $\lambda = 10.6\,\mu$m, the path length $z = 6$ km, the structural constant $C_n^2 = 10^{-15}$ cm$^{-2/3}$, the external scale of turbulence $L_0 = 1$ m, the internal scale $l_0 = 1$ cm, the number of screens used in the model is $J = 20$. The intensities on isophotes are given relative to the peak intensity of the incident beam.

shown at a distance of $z = 0.5L_{\rm df}$ [176]. The initial beam had a Gaussian profile and a plane wave front. This realization corresponds to the instant detection of the intensity at the beam cross section. One can see that fluctuations of the refractive index in the path resulted in the formation of speckles of the irregular shape.

4.2 Beam spatial statistics

4.2.1 Pulsed radiation. An investigation of the spatial statistics of the light beam in the turbulent atmosphere at nonstationary thermal self-action by the MCM represents a problem in the five-dimensional space of time t, three spatial coordinates x, y, z, and the Monte Carlo variable i. An individual realization of the field in the case $t_{\rm p} < \tau_v$ is described by system of equations (4.2) at $v = 0$.

Detailed analysis of the change in the spatial coherence upon emission of the short pulse ($\tau_{\rm s} < t_{\rm p} < \tau_v$) was carried out in [122] for a two-dimensional model of the beam in the atmosphere with the Kármán turbulence spectrum (2.53). The change of the degree of spatial coherence $\gamma(-r/2, r/2, t)$ in time was determined from the sampling of $N = 300$ dynamic realizations obtained for an ensemble of stationary, statistically independent chains of phase screens simulating small-scale fluctuations of the refractive index in the atmosphere. At the pulse leading edge ($R(t) = 0$), the nonlinear refraction is absent and the behaviour of the coherence radius calculated at the e^{-1} level of the function $|\gamma(-r/2, r/2, t)|$ corresponds to estimates [123] for a linear case.

Under conditions of the nonlinear refraction, the coherence of the light field changes nonmonotonically with time, as in the case of a beam scattered from a phase screen upon the self-action in a regular medium. At the pulse leading edge, $r_{\rm c}(t)$ increases because of the nonlinear divergence of the beam and defocusing of the induced inhomogeneities of the light field (Fig. 17). Then, with the appearance of caustics in the path of the light upon increasing the optical strength of induced thermal lenses, the fragmentation of speckles occurs and the coherence of the light field deteriorates.

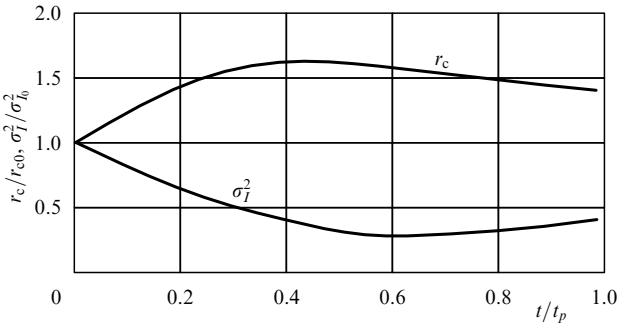

Figure 17. Relative temporal variations of the coherence radius $r_{\rm c}/r_{\rm c0}$ and the intensity variance $\sigma_I^2/\sigma_{I_0}^2$ on the beam axis upon nonstationary thermal self-action in the turbulent atmosphere. The initial radius of a Gaussian collimated beam is $a_0 = 0.1$ m, the peak intensity $I_0 = 10^3$ W/cm^2, the pulse duration $t_{\rm p} = 2 \times 10^{-2}$ s, the wavelength $\lambda = 10.6\,\mu$m, the structural turbulent constant $C_\varepsilon^2 = 4 \times 10^{-16}$ cm$^{-2/3}$, the external scale $L_0 = 0.5$ m, the internal scale $l_0 = 0.5$ cm, the absorption coefficient $\alpha_{\rm abs} = 1.4 \times 10^{-4}$ m^{-1}, the path length $z = 0.15ka_0^2$ ($\sigma_I^2 = 100$, $R(t_{\rm p}) = 150$) [122].

With the development of speckles of the light field, an increase in the intensity fluctuations is observed after their decrease caused by nonlinear defocusing at the pulse leading edge (Fig. 17). The time $t_{\rm cr}$ at which $r_{\rm c}$ and σ_I^2 begin to decrease and increase, respectively, can be estimated, as in the case of a partially coherent beam in a regular medium, from the condition that the energy transferred through a speckle inhomogeneity of the field achieves a critical value. For parameters under study, the estimate yields $t_{\rm cr} = 0.4t_{\rm p}$.

The change in time of statistical parameters of the initially coherent beam upon thermal self-action in the turbulent atmosphere is weaker as a whole than that of the partially coherent beam in a regular medium. This is explained by the fact that the additive contribution of statistically independent fluctuations of a medium may depress the mutual correlation between perturbations of the light field and medium.

4.2.2 Wind refraction. A random realization of the light field in the case of a long pulse is described by system of equations (4.2) and (4.3), in which the velocity v of the wind flow is assumed constant. The nonlinear statistical problem contains the turbulence parameter σ_J^2 (4.4), the path length $z/L_{\rm df}$, the optical thickness αz, and the nonlinearity parameter R [(4.5) and (4.7)].

The instant intensity distribution in individual realizations changes randomly at the beam cross section against the background crescent-shaped beam profile typical for a regular wind refraction (Fig. 18a) [77].

Fluctuations of the light field in the wind flow produced by the atmosphere are carried away through the beam cross section by accumulating the nonlinear perturbation $\varepsilon_{\rm nl}$ in the medium. As a result, thermal defocusing smooths off the light-field inhomogeneities in the near-axis region of the beam. The field fluctuations can increase downstream of the wind flow at sufficiently high radiation powers because of the aberration nature of a strong thermal defocusing. This is demonstrated in Fig. 18b by the profile of the scintillation

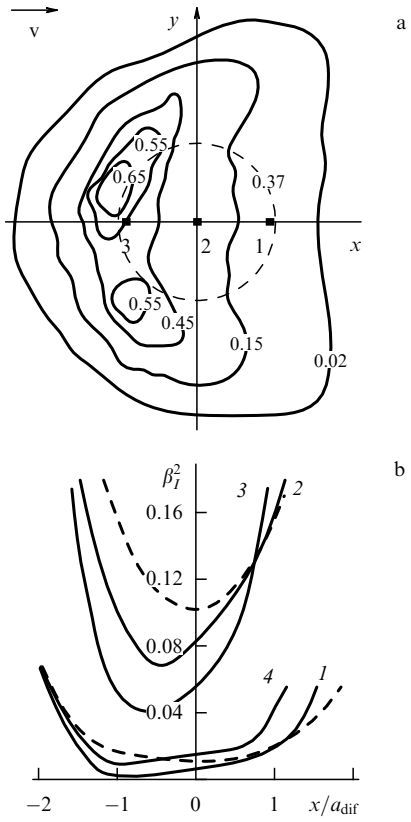

Figure 18. Wind refraction of a collimated Gaussian beam in the turbulent atmosphere in the path of length $z = 0.3L_{\text{df}}$ for the ratio of turbulence scales $L_0/l_0 = 18$ and wind velocity $v = 10$ m/s. The absorption coefficient $\alpha_{\text{abs}} = 1.4 \times 10^{-4}$ m^{-1}, the beam radius $a_0 = 6l_0$, and the wavelength $\lambda = 10.6\,\mu$m: (a) isophotes at the beam cross section for a random realization at $C_\varepsilon^2 = 10^{-16}$ cm$^{-2/3}$ and the initial peak intensity $I_0 = 380$ W cm^{-2} ($\sigma_J^2 = 0.4$, $R_v = 28$); the diffraction beam size a_{dif} is shown by the dashed circle; (b) profile of the scintillation index at the beam cross section parallel to the wind velocity; $R_v = 0$ (dashed lines), 28 (*1*, *3*), 23 (*2*), $\sigma_J^2 = 0.4$ (*1*) and 1.4 (*2*, *3*). Curve *4* is obtained from the average temperature profile [77].

index β_I^2 at the cross section of a beam parallel to the direction of the wind velocity†:

$$\beta_I^2(r, z) = \frac{\sigma_I^2(r, z)}{\langle I(r, z)\rangle} . \tag{4.8}$$

In focused beams, the power density increases with the distance and the nonlinear enhancement of the intensity fluctuations is more pronounced [80]. This allows one to estimate the critical power of a beam above which the small-scale fluctuations of the light field increase and the average value of the maximum radiation intensity in the detection plane decreases.

The development of small-scale perturbations of the light field in the direction of the wind flow is confirmed by the study of spatial coherence [77]. In the direction parallel to the flow, the scale of the field coherence on leeward of the beam drops because of the nonlinear enrichment of the spatial spectrum by high-frequency harmonics. In the direction perpendicular to the flow, the correlation between the field and intensity fluctuations is improved in this part of the beam because of its thermal defocusing. As a result, the light field of the beam under conditions of the wind refraction in the turbulent atmosphere becomes statistically anisotropic and inhomogeneous.

The inertial nature of the thermal nonlinearity justifies the use of the procedure of moments splitting for obtaining a closed equation for the field coherence function [11, 177]. However, detailed analysis has shown [77] that the introduction of the average temperature field breaks the feedback for intensity fluctuations upon thermal self-action. This leads to deterioration of the local defocusing of intensity outbursts, resulting in the enhancement of the scintillation index (Fig.18b).

4.2.3 Wind-velocity pulsations. According to [178], the spatial, L_v, and temporal, T_v, fluctuation scales of the wind-velocity components in a horizontal path of the light satisfy the conditions

$$L_v \gg a_0 , \qquad T_v \gg \tau_v . \tag{4.9}$$

It follows from the first condition that the wind-flow velocity at the beam cross section is virtually constant. The second inequality implies that in the case of quasi-continuous radiation at $t_{\text{p}} > T_v$, it is highly probable that a temperature field is established in the beam for some random distribution of the wind velocity and the propagation of radiation can be considered stationary.

The steady-state thermal self-action of the beam in the case of the random wind velocity in the path is described by system of equations (4.2), where $\tilde{\varepsilon} = 0$, $\partial T/\partial t = 0$, and $v(z)$ is a random function. In the locally isotropic turbulence field, the longitudinal, v_x, and vertical, v_y, components of the velocity have the normal distribution law. In this case, the random field of the wind velocity can be assumed as δ-correlated in the direction of light propagation.

The computer realization within this approach corresponds to the detection of the light field in the case of steady-state propagation of the beam along a path with the 'frozen' random distribution of the wind velocity. Statistical parameters of the light beam are determined by processing an ensemble of such detections obtained in time intervals $t > T_v$, when distributions of the wind velocity in the path of the light become statistically independent. The nonstationary model of thermal self-action of a beam upon turbulent mixing by a random wind flow was suggested in [179], where the three-dimensional velocity field was constructed without restrictions (4.9).

As numerical experiments show [23, 75, 79, 180], pulsations of the wind velocity decrease nonlinear distortions of a beam in the atmosphere. A random orientation of the velocity of the transverse wind flow results in irregular changes in the path of the gradient vector direction for the temperature field induced in the medium. For this reason, nonlinear distortions of the beam are not accumulated along the path. The distribution of the average intensity over the beam cross section becomes more symmetrical as compared to that for the nonlinear refraction in the case of the regular wind velocity. The suppression of nonlinear distortions is especially strongly manifested in focused beams (Fig. 19) [79].

The intensity distribution over a beam propagating in the direction of the average wind velocity is, on average,

† Notice that in the case of a long pulse, the light field is statistically stationary at $t > 3\tau_v$ and its parameters can be determined by time averaging.

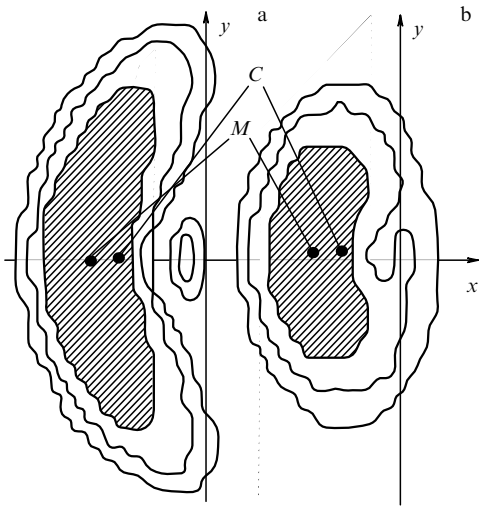

Figure 19. Distribution of the average intensity $\langle I(x, y)\rangle_N$ in the focal plane of a Gaussian beam upon wind refraction under conditions of wind-velocity pulsations. The path length is $z = 0.3L_{\rm df}$, the nonlinearity parameter $R_v = 64$, the relative variance of the wind-velocity components in the plane perpendicular to the propagation direction $\sigma_v^2 = 0.4$, the number of realizations $N = 100$. Points M and C indicate positions of the maximum intensity $\max\langle I\rangle$ in (a) the absence of pulsations ($\sigma_v^2 = 0$) and (b) for $\sigma_v^2 = 0.4$ [79].

axisymmetric provided the dispersions of the wind-velocity components at the beam cross section are coincident. As the nonlinearity increases, so does the average radius of the beam, similarly to the stationary defocusing in a heat conducting medium. This allows one to reduce the statistical problem on the average width of the beam propagating along the average wind flow to the determinate problem on the thermal defocusing in a medium with the efficient coefficient of the turbulent thermal conductivity [78]:

$$\chi_{\rm T} \simeq 1.5\, a_0 \sigma_v\,. \tag{4.10}$$

4.3 Adaptive compensation for distortions

The problem on reducing distortions of the light beams upon their formation and propagation is of great importance in modern optics. The most promising are adaptive optics systems which can correct the wave front of the beam in real time [181, 182]. With the advent of adaptive telescopes with laser star lighthouses, the resolution of astronomical observations was qualitatively improved [183, 184].

4.3.1 Models of adaptive optics systems. Theoretical analysis of adaptive systems is based on the models that involve the model of formation and propagation of radiation in a random medium, the model of a detector and a corrector of the wave front, and, finally, the control algorithm which closes the feedback loop in the system. Computer models of adaptive systems in atmospheric optics allow one to write a scenario of radiation propagation along the horizontal, inclined or vertical paths in accordance with optical models of the atmosphere for a given geographic region [185, 186]. Under conditions of the adaptive control, the light beam at the transmission aperture $z = 0$ in system (4.2) is specified as follows:

$$E(\mathbf{r}, 0, t) = E_0(\mathbf{r}, t) \exp\{\mathrm{i}U(\mathbf{r}, t)\}\,, \tag{4.11}$$

where $U(\mathbf{r}, t)$ is the controllable wave front, which is formed by a phase corrector.

According to the control basis, zonal systems are distinguished, which reproduce the phase $U(\mathbf{r}, t)$ at a number of the aperture points, and modal systems in which the phase $U(\mathbf{r}, t)$ is represented as a superposition of the Zernike polynomials describing aberrations of optical systems [see (2.64)].

The control algorithms are divided into two main classes: the aperture probing and phase conjugation [181, 182]. In the aperture probing systems, the phase $U(\mathbf{r}, t)$ is defined from the condition that the chosen 'objective function' achieves a maximum in the observation plane z_0 (for example, radiation power incident on a given aperture). The phase conjugation systems are based on the reversibility principle. Information on phase perturbations along the path is carried by the wave $\psi(\mathbf{r}, z, t)$ scattered from a flashing point in the observation plane z_0 or a laser lighthouse [183, 184], or by the reference radiation propagating along the channel of the incident beam in the opposite direction relative to a transmission aperture.

The efficiency of the adaptive systems is estimated, along with realizations of the light field at short exposures of the image, from statistical parameters obtained by the MCM, which corresponds to a long exposure in the detection plane. In papers [187, 188], the long-exposure scattering function of a point of the adaptive telescope with the Hartmann detector of the wave front was investigated.

4.3.2 High-power beams in the atmosphere. In the case of the beams propagating under conditions of the nonlinear refraction, methods of adaptive optics are primarily intended to enhance the efficiency of the laser radiation energy transfer along atmospheric paths. Because a random walk and irregular defocusing of the beam in a random wind flow mainly result in a decrease in the power density on a receiving aperture, the compensation for these perturbations is the most important problem of adaptive optics systems. The wind refraction is mainly determined by the first- and second-order phase aberrations, which can be compensated by means of the modal correction with a comparatively small number (no more than ten) of control channels [189, 190].

The modal control of the beam phase based on the maximization of the 'objective function' was considered in the quasi-stationary approximation ($T_v \gg \tau_v$) in Ref. [191]. The dynamic compensation for irregular distortions caused by pulsations of the wind velocity at $T_v \geqslant \tau_v$ was studied in [192]. It was shown that as the radiation power and period of velocity pulsations increase, the efficiency of the adaptive control of the beam phase grows as compared to that for its *a priori* correction based on averaged parameters of the irregular atmosphere. Computer simulation of the transient process of the beam dynamic focusing upon wind refraction in the atmosphere with 'frozen' turbulence was carried out in Refs [81, 193, 194].

The enhancement of stability of the adaptive focusing of a high-power beam in the turbulent atmosphere was considered in a series of papers [195 – 197], where the algorithm of the phase control based on the simplex method was developed. In the case of dynamic focusing of a beam under conditions of wind-velocity pulsations, this algorithm is stable up to the velocity variance $\sigma_v \simeq 0.25v_0^2$, whereas a standard gradient procedure of searching for a maximum of the 'objective function' becomes unstable for $\sigma_v^2 \simeq 0.1v_0^2$. In these papers, the efficiency of the adaptive control of the beam phase was studied by the MCM in the case of nonlinear refraction under

conditions of the simultaneous effect of wind-velocity pulsations and large-scale fluctuations of the refractive index in the path. It was demonstrated that the radiation energy $W(t)$, averaged over the sampling, incident during the time $t = 12\tau_v$ on a receiving aperture is approximately 30% greater than the energy $W_0(t)$ in the absence of the control (Fig. 20).

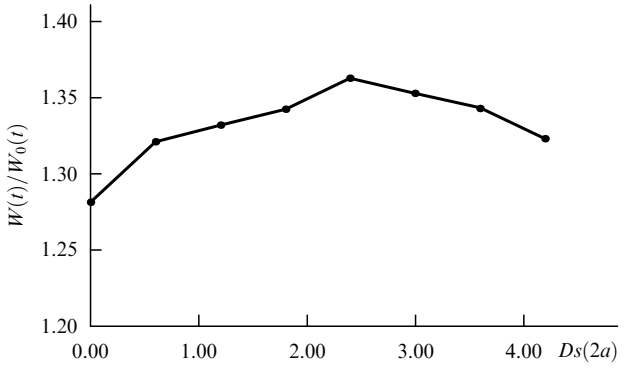

Figure 20. Relative increase in the averaged radiation energy $W(t)/W_0(t)$ on a receiving aperture in the case of the adaptive simplex-method control of the phase of a beam propagating under conditions of nonlinear refraction caused by wind-velocity pulsations and large-scale fluctuations of the refractive index. The path length is $z = 0.5L_{\text{df}}$ [211]. $Ds(2a)$ was defined in [123].

The efficiency of correction of turbulent and nonlinear distortions in the case of short pulses was numerically examined in [198] for the system of wave-front reversal.

The results of studies on the adaptive correction of distortions of a high-power laser beam in the turbulent atmosphere are presented in [82] for the example of imaginary scenario of the laser antimissile defence. The point-by-point control of the beam phase was considered on the basis of the phase conjugation algorithm. It was found for specific radiation parameters and conditions in the high-altitude atmospheric path, that the turbulence on average depresses the attenuation of the radiation intensity at the end of the path caused by the nonlinear refraction. This results from the turbulent spreading of the thermal field gradients induced in the beam channel. The adaptive compensation of the distortions based on the phase conjugation algorithm results in a stronger manifestation of the thermal self-action than in the absence of the control of the high-power beam phase in the turbulent atmosphere.

5. Conclusions

In this review, the basic concepts of statistical tests in nonlinear optics of random (randomly inhomogeneous) media were considered. It is not accidentally that a significant attention was paid to the substantiation of the phase screen model for a random nonlinear medium and of the method of computer experiments with random waves, because this determines to a large degree the reliability of results obtained by the Monte Carlo method. The generality of the phase screen model for random nonlinear media permits its application to studying the propagation of sound waves in the ocean and atmosphere, seismic waves in the Earth's crust, and the electromagnetic radiation in the ionosphere, space, and biological tissues.

The review does not concern statistical problems of laser physics, which are related to the formation of radiation in lasers, analysis of the lasing stability, and the sensitivity of laser systems to parameter variations. Problems of the statistical study of the effect of the laser radiation on a substance, surface, and complex molecules could be the subject of a separate review.

Acknowledgments. The author thanks his colleagues S S Chesnokov and S A Shlenov for useful discussions and I V Pashkova for her great help in preparation of this review. The author also expresses his deep gratitude to I A Yakovlev for his attention to this work. This work was partially supported by the European Research Office, contract No. 68171-94-C-9147, London, UK.

References

1. Akhmanov S A, D'yakov Yu E, Chirkin A S *Vvedenie v Statisticheskuyu Radiofiziku i Optiku* (Introduction to Statistical Radiophysics and Optics) (Moscow: Nauka, 1981)
2. New J H J *Proc. IEEE* **67** 380 (1979)
3. Bespalov V I, Litvak A G, Talanov V I, in *Nelineĭnaya Optika* (Nonlinear Optics) (Novosibirsk: Nauka, 1968)
4. Sherstobitov V E *Izv. Akad. Nauk SSSR Ser. Fiz.* **46** 1905 (1982) [*Bull. Acad. Sci. USSR, Phys. Ser.*]
5. Zuev V E, Zemlyanov A A, Kopytin Yu D *Nelineĭnaya Optika Atmosfery* (Nonlinear Atmospheric Optics) (Leningrad: Gidrometeoizdat, 1989)
6. Weiland J, Wilhelmsson H *Coherent Nonlinear Interaction of Waves in Plasmas* (Oxford, New York: Pergamon Press, 1977) [Translated into Russian (Moscow: Energoizdat, 1981)]
7. Kadomtsev B B, Petviashvili V I *Dokl. Akad. Nauk SSSR* **208** 794 (1973) [*Sov. Phys. Dokl.* **18** 115 (1973)]
8. Rudenko O V *Usp. Fiz. Nauk* **149** 413 (1986) [*Sov. Phys. Usp.* **29** 620 (1986)]
9. Gurbatov S N, Malakhov A N, Saichev A I *Nelineĭnye Sluchaĭnye Volny v Sredakh bez Dispersii* (Nonlinear Random Waves in Nondispersive Media) (Moscow: Nauka, 1990) [Translated into English (Manchester, New York: Univ. Press, Martin Press, 1991)]
10. Kandidov V P *Izv. Akad. Nauk SSSR Ser. Fiz.* **49** 442 (1985) [*Bull. Acad. Sci. USSR, Phys. Ser.* **49** 24 (1985)]
11. Vorob'ev V V *Teplovoe Samovozdeĭstvie Lazernogo Izlucheniya v Atmosfere* (Thermal Self-Action of Laser Radiation in the Atmosphere) (Moscow: Nauka, 1987)
12. Liou L W, Cao X D, McKinstrie C J, Agrawal G P *Phys. Rev. A* **46** 4202 (1992)
13. Gochelashvili K S, Chashei I V, Shishov V I *Kvantovaya Elektron.* **7** 666 (1980) [*Sov. J. Quantum Electron.* **10** 1207 (1980)]
14. Babichenko S M, Kandidov V P *Vestn. Mosk. Univ. Ser. Fiz. Astron.* **26** 43 (1985) [*Moscow Univ. Phys. Bull.* **40** 48 (1985)]
15. Pasmanik G A *Zh. Eksp. Teor. Fiz.* **66** 490 (1974) [*Sov. Phys. JETP* **39** 234 (1974)]
16. Betin A A, Pasmanik G A *Izv. Vyssh. Uchebn. Zaved. Radiofiz.* **20** 1534 (1977) [*Radiophys. Quantum Electron.*]
17. Banakh V A, Smalikho I N *Kvantovaya Elektron.* **14** 2098 (1987) [*Sov. J. Quantum Electron.* **17** 1341 (1987)]
18. Fattakhov A M, Chirkin A S *Kvantovaya Elektron.* **10** 1989 (1983) [*Sov. J. Quantum Electron.* **13** 1326 (1983)]
19. Chirkin A S, Yusubov F M *Vestn. Mosk. Univ. Ser. Fiz. Astron.* **26** 57 (1985) [*Moscow Univ. Phys. Bull.* **40** 66 (1985)]
20. Vlasov V A, Petrishchev V A, Talanov V I *Izv. Vyssh. Uchebn. Zaved. Radiofiz.* **14** 1353 (1971) [*Radiophys. Quantum Electron.*]
21. Vysloukh V A, Fattakhov A M *Izv. Vyssh. Uchebn. Zaved. Radiofiz.* **29** 545 (1986) [*Radiophys. Quantum Electron.* **29** 404 (1986)]
22. Fleck J A, Morris J R, Feit M D *Appl. Phys.* **10** 129 (1976)
23. Egorov K D, Kandidov V P, Chesnokov S S *Izv. Vyssh. Uchebn. Zaved. Fiz.* **26** 66 (1983) [*Sov. Phys. J.* **26** 161 (1983)]
24. Taha T R, Ablowitz M J *J. Comput. Phys.* **55** 203 (1984)

25. Shreider Yu A (Ed.) *Metod Statisticheskikh Ispytaniĭ* (Metod Monte-Karlo) [Method of Statistical Tests (Monte Carlo Method)] (Moscow: Fizmatgiz, 1962) [Amsterdam, New York: Elsevier, 1964]
26. Aleshkevich V A, Kozhoridze G D, Matveev A N *Usp. Fiz. Nauk* **161** (9) 81 (1991) [*Sov. Phys. Usp.* **34** 777 (1991)]
27. Kandidov V P *Izv. Akad. Nauk. SSSR Ser. Fiz.* **47** 1583 (1983) [*Bull. Acad. Sci. USSR, Ser.* **47** 120 (1983)]
28. Basov N G et al. *Zh. Eksp. Teor. Fiz.* **56** 1546 (1969) [*Sov. Phys. JETP* **29** 830 (1969)]
29. Fleck J A (Jr) *J. Appl. Physics* **39** 3318 (1968)
30. Zel'dovich B Ya, Kuznetsova T I *Usp. Fiz. Nauk* **106** (1) 47 (1972) [*Sov. Phys. Usp.* **15** 25 (1972)]
31. Lariontsev E G, Serkin V N *Izv. Vyssh. Uchebn. Zaved. Radiofiz.* **22** 425 (1979) [*Radiophys. Quantum Electron.* **22** 293 (1979)]
32. Isaev S K et al. *Zh. Eksp. Teor. Fiz.* **79** 1239 (1980) [*Sov. Phys. Usp.* **52** 626 (1980)]
33. *Metod Monte-Karlo v Atmosfernoĭ Optike* (Monte Carlo Method in Atmospheric Optics) (Novosibirsk: Nauka, 1976)
34. Eflov V B, Il'inskiĭ Yu A *Vestn. Mosk. Univ. Ser. Fiz. Astron.* **25** 115 (1984) [*Moscow Univ. Phys. Bull.* **39** 121 (1984)]
35. Zuev V E, Banakh V A, Pokasov V V *Optika Turbulentnoĭ Atmosfery* (Optics of the Turbulent Atmosphere) (Leningrad: Gidrometeoizdat, 1988)
36. Davis J M, Mckee Th B, Cox S K *Appl. Opt.* **24** 3193 (1985)
37. Valley M T *Proc. SPIE* **1688** 73 (1992)
38. Akimov P I, Baskakov S I *Trudy 4 Vsesoyuznogo Simpoziuma po Rasprostraneniyu Lazernogo Izlucheniya v Atmosfere* (Proceedings of the 4th All-Union Symposium on Propagation of Laser Radiation in the Atmosphere, Tomsk, 1977) p. 224
39. Ewart T E *J. Acoust. Soc. Am.* **67** 496 (1980)
40. Rytov S M, Kravtsov Yu A, Tatarskiĭ V I *Vvedenie v Statisticheskuyu Radiofiziku* Ch. 2 (Introduction to Statistical Radiophysics) Part 2 (Moscow: Nauka, 1978) [Translated into English (Berlin, New York: Springer-Verlag, 1987)]
41. Prokhorov A M et al. *Usp. Fiz. Nauk* **114** (11) 415 (1974) [*Sov. Phys. Usp.* **17** 826 (1975)]
42. Chernov L A *Volny v Sluchaĭno-neodnorodnykh Sredakh* (Waves in Randomly Inhomogeneous Media) (Moscow: Nauka, 1975) [New York: McGraw-Hill, 1960]
43. Kravtsov Y A *Rep. Prog. Phys.* **55** 39 (1992)
44. Bramley E N *Proc. Roy. Soc. A* **225** 515 (1954)
45. Ratcliffe J A *Rep. Phys.* **19** 188 (1956)
46. Salpeter E E *Astrophys. J.* **147** 433 (1964)
47. Bramley E N *J. Atmos. Terr. Phys.* **39** 367 (1977)
48. Rino C L *Radio. Sci.* **15** 41 (1980); **17** 855 (1982)
49. Shishov V I *Izv. Vyssh. Uchebn. Zaved. Radiofiz.* **14** 85 (1971)
50. Yakushkin I G *Izv. Vyssh. Uchebn. Zaved. Radiofiz.* **17** 1350 (1974) [*Radiophys. Quantum Electron.*]
51. Frankenthal S, Whitman A M *JOSA A* **6** 1827 (1989)
52. Rudenko O V, Khokhlova V A *Akust. Zh.* **40** 126 (1994) [*Acoustical Phys.* **40** 593 (1994)]
53. Codona J L et al. *Phys. Rev. Lett.* **55** 9 (1985)
54. Booker H G, Ferguson J A, Vats H O *J. Atmos. Terr. Phys.* **47** 381 (1985)
55. Erukhimov L M, Uryadov V P *Izv. Vyssh. Uchebn. Zaved. Radiofiz.* **11** 1852 (1968)
56. Uscinski B J *JOSA A* **2** 2077 (1985)
57. Shen Y R *Principles of Nonlinear Optics* (New York: J. Wiley, 1984) [Translated into Russian (Moscow: Nauka, 1989)]
58. Kandidov V P, in *Nelineĭnaya Optika i Optoakustika Atmosfery* (Nonlinear Optics and Optoacoustics of the Atmosphere) (Tomsk, 1988) p. 29
59. Akhmanov S A, Vysloukh V A, Chirkin A S *Optika Femtosekundnykh Lazernykh Impul'sov* (Optics of Femtosecond Laser Pulses) (Moscow: Nauka, 1988) [Translated into English (New York: AIP, 1992)]
60. Egorov K D et al. *Kvantovaya Elektron.* **12** 1825 (1985) [*Sov. J. Quantum Electron.* **15** 1208 (1985)]
61. Ermakov S M, Mikhailov G A *Kurs Statisticheskogo Modelirovaniya* (Course of Statistical Modelling) (Moscow: Nauka, 1976)
62. Buckley R *J. Atmos. Terr. Phys.* **37** 1431 (1975)
63. Valley G C, Brown W P *Appl. Optics* **21** 3002 (1982)
64. Wernik A W, Lin C H, Yen K C *Radio Sci.* **15** 559 (1980)
65. Knepp D L *Proc. IEEE* **71** 722 (1983)
66. Uscinski B J, in *Wave Propagation in Random Media* (SPIE, PM-09, 1992) p. 346
67. Flatte St M, Tappert F D *J. Acoust Soc. Am.* **58** 1151 (1975)
68. Martin J M, Flatte S M *Applied Optics* **27** 2111 (1988)
69. Martin J M, Flatte S M *J. Opt. Soc. Am. A* **7** 838 (1990)
70. Flatte S M, Wang G Y, Martin J M *J. Opt. Soc. Am. A* **10** 2363 (1993)
71. Dashen R et al. *J. Opt. Soc. Am. A* **10** 1233 (1993)
72. Flatte S M, Bracher Ch, Wang G Y *J. Opt. Soc. Am. A* **11** 2080 (1994)
73. Gribova E Z, Saichev A I *Radiotekh. Radioelektron.* **39** 193 (1994) [*J. Commun. Electron.* **39** 1 (1994)]
74. Macaskill C, Ewart T E *IMA J. Appl. Math.* **33** 1 (1984)
75. Konyaev P A, Lukin V P *Izv. Vyssh. Uchebn. Zaved. Fiz.* **26** 79 (1983) [*Sov. Phys. J.* **26** 173 (1983)]
76. Kandidov V P, Lednev V I *Kvantovaya Elektron.* **8** 837 (1981) [*Sov. J. Quantum Electron.* **11** 521 (1981)]
77. Kandidov V P, Shlenov S A *Kvantovaya Elektron.* **12** 1490 (1985) [*Sov. J. Quantum Electron.* **15** 982 (1985)]
78. Egorov K D, Kandidov V P, Laguchev A S *Izv. Vyssh. Uchebn. Zaved. Radiofiz.* **26** 1175 (1983)
79. Konyaev P A, Lukin V P *Kvantovaya Elektron.* **15** 341 (1988) [*Sov. J. Quantum Electron.*]
80. Zuev V E, Konyaev P A, Lukin V P *Izv. Vyssh. Uchebn. Zaved. Fiz.* **28** 6 (1985) [*Sov. Phys. J.* **28** 859 (1985)]
81. Vysloukh V A et al. *Izv. Vyssh. Uchebn. Zaved. Fiz.* **28** 30 (1985) [*Sov. Phys. J.* **28** 878 (1985)]
82. Gebhardt Fr G *Proc. SPIE* **2120** 76 (1994)
83. Godunov S K, Ryabenskiĭ V S *Raznostnye Skhemy* (Difference Schemes) (Moscow: Nauka, 1977) [Translated into English (Amsterdam, New York: Elsevier, 1987)]
84. Hardin R H, Tappert F D *SIAM Review* **15** 423 (1973)
85. Martin J, in *Wave Propagation in Random Media* (SPIE, PM-09, 1992) p. 463
86. Fisher R A, Bischel W K *J. Appl. Phys.* **46** 4921 (1975)
87. Agrawal G P *Nonlinear Fiber Optics* (New York: Academic Press, 1989) [Translated into Russian (Moscow: Mir, 1996)]
88. Fedorov S V, Yur'ev M S *Kvantovaya Elektron.* **17** 881 (1990) [*Sov. J. Quantum Electron.* **20** 801 (1990)]
89. Elkin N N, Napartovich A P *Prikladnaya Optika Lazerov* (Applied Laser Optics) (Moscow: TsNII Atominform, 1989)
90. Fleck J F, Morris J R, Bills E S *IEEE J.* **QE-14** 353 (1978)
91. Chang R S F, Lehmberg R H, Duignan M T, Djeu N *IEEE J.* **QE-21** 477 (1985)
92. Kandidov V P, Kurlyandtsev M Yu *Izv. Ross. Akad. Nauk Ser. Fiz.* **56** 35 (1992)
93. Volkova E A *Izv. Akad. Nauk SSSR Ser. Fiz.* **50** 804 (1989)
94. Potter D *Computational Physics* (New York: Wiley, 1973) [Translated into Russian (Moscow: Mir, 1975)]
95. Thomson D J, Chapman N R *J. Acoust. Soc. Am.* **74** 1848 (1983)
96. Haines E M *J. Comp. Phys.* **60** 353 (1985)
97. Kandidov V P, Shlenov S A, in *Proc. Eight Intern. School of Coherent Optics* (Bratislava, 1987) p. 26
98. Tatarskiĭ V I *Teoriya Fluktuatsionnykh Yavleniĭ pri Rasprostranenii Voln v Turbulentnoĭ Atmosfere* (Theory of Fluctuation Phenomena upon Propagation of Waves in the Turbulent Atmosphere) (Moscow: Izd. Akad. Nauk SSSR, 1959)
99. Ishimaru A *Wave Propagation and Scattering Media* (New York: Academic Press, 1978) [Translated into Russian (Moscow: Mir, 1981)]
100. Kandidov V P, Ledenev V I *Vestn. Mosk. Univ. Ser. Fiz. Astron.* **23** 3 (1982)
101. Bykov V V *Tsifrovoe Modelirovanie v Statisticheskoĭ Radiofizike* (Numerical Simulation in Statistical Radiophysics) (Moscow: Sovetskoe Radio, 1971)
102. Mirkin L I, Rabinovich M A, Yaroslavskiĭ L I *Zh. Vychisl. Mat. Mat. Fiz.* **12** 1353 (1972) [*USSR Comput. Math. Math. Phys.*]
103. Rabiner L, Gold B *Theory and Application of Digital Signals Processing* (Englewood Cliffs: Prentice-Hall, 1975) [Translated into Russian (Moscow: Mir, 1978)]
104. Goldring Th, Carlson L *Proc. SPIE* **1060** 244 (1989)

105. Mironov V L *Rasprostranenie Lazernogo Izlucheniya v Turbulentnoĭ Atmosfere* (Propagation of Laser Radiation in the Turbulent Atmosphere) (Novosibirsk: Nauka, 1981)
106. Kandidov V P, Ledenev V I *Izv. Vyssh. Uchebn. Zaved. Radiofiz.* **24** 438 (1981)
107. Noll R J *J. Opt. Soc. Am.* **66** 207 (1976)
108. Wang J Y, Markey J K *J. Opt. Soc. Am.* **68** 78 (1978)
109. Fried D L *Proc. IEEE* **55** 57 (1967)
110. Kandidov V P, Shlenov S A *Trudy 10 Vsesoyuznogo Simpoziuma po Rasprostraneniyu Lazernogo Izlucheniya v Atmosfere* (Proceedings of the 10th All-Union Symposium on Propagation of Laser Radiation in the Atmosphere, Tomsk, 1989) p. 142
111. Tel'pukhovskiĭ I E, Chesnokov S S *Opt. Atmos. Okeana* **4** 1294 (1991)
112. Roddier N *Optical Eng.* **29** 1174 (1990)
113. Aksenov V P, Isaev Yu N *Opt. Atmos. Okeana* **7** 947 (1994)
114. Aksenov V P et al. *Opt. Atmos. Okeana* **7** 955 (1994)
115. Kandidov V P, Shlenov S A, in *Proc. 8th Laser Optics Conf.* (St. Petersburg, 1995) p. 48
116. Herman B J, Strugala L A *Proc. SPIE* **1221** 183 (1990)
117. Lane R G, Glindemann A, Dainty J C, in *Waves in Random Media* **2** (3) 209 (SPIE, 1992)
118. Johansson E M, Gavel D T *Proc. SPIE* **2200** 372 (1994)
119. Volkova E A, in *Lazernye Puchki. Rasprostranenie v Sredakh i Upravlenie Parametrami* (Laser Beams: Propagation in Media and Control of Parameters) (Khabarovsk, 1985) p. 50
120. McCumber D E *Bell. Syst. Techn. J.* **44** 333 (1965)
121. Petrishchev V A *Izv. Vyssh. Uchebn. Zaved. Radiofiz.* **14** 1416 (1971)
122. Kandidov V P, Shlenov S A *Trudy 6 Vsesoyuznogo Simpoziuma po Rasprostraneniyu Lazernogo Izlucheniya v Atmosfere* (Proceedings of the 6th All-Union Symposium on Propagation of Laser Radiation in the Atmosphere, Tomsk, 1981) part 3, p. 199
123. *Lazernoe Izluchenie v Turbulentnoĭ Atmosfere* (Laser Radiation in the Turbulent Atmosphere) (Moscow: Nauka, 1976)
124. Kandidov V P, Shlenov S A *Izv. Vyssh. Uchebn. Zaved. Radiofiz.* **27** 1158 (1984) [*Radiophys. Quantum Electron.* **27** 817 (1984)]
125. Vinogradova M B, Rudenko O V, Sukhorukov A P *Teoriya Voln* (Theory of Waves) (Moscow: Nauka, 1990)
126. Aleshkevich V A et al. *Kvantovaya Elektron.***17** 1619 (1990) [*Sov. J. Quantum Electron.* **20** 1512 (1990)]
127. Aleshkevich V A et al. *Kvantovaya Elektron.* **15** 325 (1988) [*Sov. J. Quantum Electron.* **18** 529 (1988)]
128. Aleshkevich V A, Lebedev S S, Matveev A N *Zh. Eksp. Teor. Fiz.* **83** 1249 (1982) [*Sov. Phys. JETP* **56** 715 (1982)]
129. Vysloukh V A *Usp. Fiz. Nauk* **136** 519 (1982) [*Sov. Phys. Usp.* **25** 176 (1982)]
130. Aleshkevich V A, Lebedev S S, Matveev A N *Kvantovaya Elektron.* **8** 1090 (1981) [*Sov. J. Quantum Electron.* **11** 647 (1981)]
131. Kandidov V P, Shlenov S A *Izv. Akad. Nauk SSSR Ser. Fiz.* **50** 1191 (1986) [*Bull. Acad. Sci. USSR, Phys. Ser.* **50** 142 (1986)]
132. Hudson D *Statistics. Lectures on Elementary Statistics and Probability* (Geneva: 1964) (Translated into Russian (Moscow: Mir, 1967)]
133. Kandidov V P, Shlenov S A V*estn. Mosk. Univ. Ser. Fiz. Astron.* **25** 51 (1984) [*Moscow Univ. Phys. Bull.* **39** 59 (1984)]
134. Kandidov V P, Kosareva O G, Shlenov S A *Kvantovaya Elektron.* **20** 1016 (1993) [*Sov. J. Quantum Electron.* **23** 885 (1993)]
135. Fattakhov A M, Chirkin A S *Kvantovaya Elektron.* **11** 2349 (1984) [*Sov. J. Quantum Electron.* **14** 1556 (1984)]
136. Elgin J N *Phys. Lett. A* **110** 441 (1985)
137. Vysloukh V A, Ivanov A V, Cherednik I V *Izv. Vyssh. Uchebn. Zaved. Radiofiz.* **30** 980 (1987) [*Radiophys. Quantum Electron.* **30** 728 (1987)]
138. Vanagas E A, Manykin E A, Surina I I Preprint IAE 4627/1 (Moscow: Institute of Atomic Energy, 1988)
139. Akhmanov S A, Vysloukh V A, Chirkin A S *Usp. Fiz. Nauk* **149** 449 (1982) [*Sov. Phys. Usp.* **29** 642 (1986)]
140. Vysloukh V A, Sukhotkova N A *Kvantovaya Elektron.* **16** 130 (1989) [*Sov. J. Quantum Electron.* **19** 85 (1989)]
141. Maimistov A I, Manykin E A, Sklyarov Yu M *Kvantovaya Elektron.* **13** 2243 (1986) [*Sov. J. Quantum Electron.* **16** 1480 (1986)]
142. Vanagas E A, Maimistov, Manykin E A Preprint IAE 4627/15 (Moscow: Institute of Atomic Energy, 1988)
143. Zakharov V E et al. *Teoriya Solitonov* (Theory of Solitons) (Moscow: Mir, 1980) [Translated into English (New York: Cons. Bureau, 1984)]
144. Vysloukh V A, Cherednik I V *Dokl. Akad. Nauk SSSR* **289** 336 (1986) [*Sov. Phys. Dokl.*]
145. Vysloukh V A, Ivanov A V *Izv. Akad. Nauk SSSR Ser. Fiz.* **52** 359 (1988) [*Bull. Acad. Sci. USSR, Phys. Ser.* **52** 126 (1988)]
146. Aleshkevich V A, Lebedev S S, Matveev A N *Kvantovaya Elektron.* **11** 459 (1984) [*Sov. J. Quantum Electron.* **14** 983 (1984)]
147. Kandidov V P, Shlenov S A *Izv. Akad. Nauk SSSR Ser. Fiz.* **52** 1232 (1988) [*Bull. Acad. Sci. USSR, Phys. Ser.* **52** 169 (1988)]
148. Rae S C, Burnett K *Phys. Rev. A* **46** 1084 (1992)
149. Kosareva O G, Shlenov S A *Izv. Ross. Akad. Nauk Ser. Fiz.* **56** 56 (1992) [*Bull. Acad. Sci. RF, Phys. Ser.*]
150. Akhmanov S A et al. *Quantum Electron.* **QE-4** 568 (1968)
151. Galich N E *Kvantovaya Elektron.* **21** 670 (1994) [*Sov. J. Quantum Electron.* **24** 618 (1994)]
152. Zel'dovich B Ya, Shkunov V V *Izv. Akad. Nauk SSSR Ser. Fiz.* **48** 1545 (1984) [*Bull. Acad. Sci. USSR, Phys. Ser.* **48** 85 (1984)]
153. Babichenko S M, Kandidov V P *Kvantovaya Elektron.* **11** 1372 (1984) [*Sov. J. Quantum Electron.* **14** 926 (1984)]
154. Galich N E, Petrushchenkov V A *Kvantovaya Elektron.* **21** 751 (1994) [*J. Quantum Electron.* **24** 703 (1994)]
155. Kandidov V P, Kosareva O G, Shlenov S A *Kvantovaya Elektron.* **21** 971 (1994) [*J. Quantum Electron.* **24** 905 (1994)]; *Nonlinear Optics* **12** 119 (1994)
156. Rae S C *Opt. Commun.* **104** 330 (1994)
157. Crenshaw M E, Cantrell C D *Phys. Rev. A* **39** 126 (1994)
158. Starostin A N et al. *Zh. Eksp. Teor. Fiz.* **108** 1203 (1995) [*JETP* **81** 660 (1995)]
159. Patrushevich Yu V, Starostin A N *Kvantovaya Elektron.* (1996) (to be published)
160. Babichenko S M et al. *Kvantovaya Elektron.* **13** 2183 (1986) [*Sov. J.Quantum Electron.* **16** 1443 (1986)]
161. Volkova E A, Kandidov V P *Kvantovaya Electron.* **16** 580 (1989) [*Sov. J. Quantum Electron.* **19** 383 (1989)]
162. D'yakov Yu E, Nikitin S Yu *Kvantovaya Elektron.* **16** 580 (1989) [*Sov. J. Quantum Electron.* **17** 1227 (1987)]
163. Rentjes J et al. *JOSA B* **3** 1408 (1986)
164. Ackerhalt J R, Kurnit N A *JOSA B* **3** 1352 (1986)
165. (Results are obtained by a student of Moscow State University Yu M Bekish)
166. Averbach V S et al. *Izv. Vyssh. Uchebn. Zaved. Radiofiz.* **21** 1077 (1978) [*Radiophys. Quantum Electron.*]
167. Gordiets B F, Osipov A I, Khokhlov R V *Zh. Tekh. Fiz.* **44** 1063 (1974) [*Sov. Phys. Tech. Phys.* **19** 669 (1974)]
168. Egorov K D, Kandidov V P, Ognev L I *Kvantovaya Elektron.* **8** 1012 (1981) [*Sov. J. Quantum Electron.* **11** 603 (1981)]
169. Basov N G et al. *Dokl. Akad. Nauk SSSR* **284** 1346 (1986) [*Sov. Phys. Dokl.* **30** 866 (1985)]
170. Smith D C *Proc. IEEE* **65** 1679 (1977)
171. Akhmanov S A et al. *Izv. Vyssh. Uchebn. Zaved. Radiofiz.* **23** 1 (1980) [*Radiophys. Quantum Electron.* **23** 1 (1980)]
172. Gordin M P, Sokolov A V, Strelkov G M, in *Rasprostranenie Moshchnogo Lasernogo Izlucheniya v Atmosfere* (Propagation of High-Power Laser Radiation in the Atmosphere) [Itogi Nauki i Tekhniki, Vyp. 20, Radiofiz. (Moscow: VINITI, 1980)] p. 206
173. *Moshchnoe Lazernoe Izluchenie v Atmosfernom Aerozole* (High-Power Laser Radiation in an Atmospheric Aerosol) (Novosibirsk: Nauka, 1984)
174. Starunov V S, Fabelinskiĭ I L *Usp. Fiz. Nauk* **98** (7) 441 (1969) [*Sov. Phys. Usp.* **12** 463 (1970)]
175. Basov N G et al. *Dokl. Akad. Nauk SSSR* **283** 1329 (1985) [*Sov. Phys. Dokl.* **30** 682 (1985)]
176. (Results are obtained by a student of Moscow State University M P Tamarov)
177. Aleshkevich V A et al. *Kvantovaya Electron.* **9** 134 (1982) [*Sov. J. Quantum Electron.* **12** 86 (1982)]
178. Lumly J, Panofsky H *The Structure of Atmospheric Turbulence* (New York: Intersience Publ., 1964) [Translated into Russian (Moscow: Mir, 1966)]
179. Wallace J *Proc. SPIE* **1408** 19 (1991)

180. Egorov K D, Kandidov V P, Laguchev A S *Trudy 6 Vsesoyuznogo Simpoziuma po Rasprostraneniyu Lazernogo Izlucheniya v Atmosfere* (Proceedings of the 6th All-Union Symposium on Propagation of Laser Radiation in the Atmosphere, Tomsk, 1981) part 3. p. 203
181. Vorontsov M A, Shmal'gauzen V I *Printsipy Adaptivnoĭ Optiki* (Principles of Adaptive Optics) (Moscow: Nauka, 1985)
182. Vitrichenko E A (Ed.) *Adaptivnaya Optika* (Adaptive Optics) (Moscow: Mir, 1980)
183. Hubin N, Nocthe L *Science* **262** 1390 (1993)
184. Tyson R K *Proc. SPIE* **2222** 404 (1994)
185. Hills L S, Long J E, Gebhardt F G *Proc. SPIE* **1408** 41 (1991)
186. Lukin V P et al. *Opt. Atmos. Okeana* **8** 409 (1995) [*Atmospheric and Oceanic Optics*]
187. Lukin V P, Maier N N, Fortes B V *Opt. Atmos. Okeana* **4** 1298 (1991); **5** 1241 (1992); **5** 1324 (1992) [*Atmospheric and Oceanic Optics*]
188. Fortes B V, Lukin V P *Proc. SPIE* **1688** 477 (1992)
189. Nahrstedt D A *Appl. Optics* **22** 244 (1983)
190. Chesnokov S S *Kvantovaya Electron.* **10** 1160 (1983) [*Sov. J. Quantum Electron.* **13** 742 (1983)]
191. Egorov K D, Chesnokov S S *Kvantovaya Electron.* **14** 1269 (1987) [*Sov. J. Quantum Electron.* **17** 808 (1987)]
192. Kanev F Yu, Chesnokov S S *Opt. Atmos.* **3** 598 (1990) [*Atmospheric Optics*]
193. Konyaev P A, Lukin V P, Mironov V L *Izv. Akad. Nauk SSSR Ser. Fiz.* **49** 536 (1985) [*Bull. Acad. Sci. USSR, Phys. Ser.* **49** 113 (1985)]
194. Chesnokov S S, Shlenov S A *Izv. Vyssh. Uchebn. Zaved. Radiofiz.* **32** 847 (1989) [*Radiophys. Quantum Electron.* **32** 631 (1989)]
195. Malafeeva I V, Tel'pukhovskiĭ I E, Chesnokov S S *Opt. Atmos. Okeana* **5** 1252 (1992) [*Atmospheric and Oceanic Optics*]
196. Malafeeva I V, Chesnokov S S *Opt. Atmos. Okeana* **6** 1490 (1992) [*Atmospheric and Oceanic Optics*]
197. Chesnokov S S, Davletshina I V *Proc. SPIE* **2222** 423 (1994); **2312** 305 (1995)
198. Vasil'ev O I et al. *Opt. Atmos. Okeana* **3** 1312 (1990) [*Atmospheric and Oceanic Optics*]